TÉCNICO LISBOA

Thermal management system of LNEG pilot area: numerical analysis and experimental validation

Volodymyr Pobuta

Thesis to obtain the Master of Science Degree in

Energy Engineering and Management

Supervisors: Prof. Carlos Augusto Santos Silva
Dr. Jorge Manuel Resende Vieira Facão

Examination Committee

Chairperson: Prof. Jorge de Saldanha Gonçalves Matos
Supervisor: Prof. Carlos Augusto Santos Silva
Member of the Committee: Dr. Rui Pedro da Costa Neto

May 2023

To my mother and father, whose love and strength inspire me every day to become a better version of myself and to uncle Yuriy, who helped me and our family to overcome the greatest of obstacles

Acknowledgments

Firstly, I would like to thank LNEG for giving me this great opportunity to work in their laboratories and to participate in a great European project such as SUDOE IMPROVEMENT. For the patience, kindness and guidance, I am in great debt to Dr.Jorge Facão, Dr.David Loureiro, Dr.João Correia and all the staff of the laboratory, which helped me through this unexpected journey.

Secondly, I would like to give my appreciation to Professor Manuel Pinheiro from Instituto Superior Técnico, with whom I have worked first before changing my subject of thesis. Despite parting ways, I truly appreciate the opportunity that he gave me to learn about building certification according to Lidera. As for Professor Carlos Silva, I am grateful for helping me during the elaboration of my new thesis and the guidance he gave me to create this scientific work.

Saving the best for last, I bow down to my parents and family, who stood by me during my lows and cheered me up during my highs. Without their sacrifices and efforts to give me a better life and future, I would have never dreamed of joining this renowned institution, far away from our home. Without their help and patience, I would have never succeeded in my academic career, nor I would have been given the privilege of learning how to live by myself, far away from the comfort of home. In the end, I dedicate this work to them, as they are the pillars of my life and upon this sturdy and unbreakable foundation, I will build my dreamed castle of knowledge, strength and integrity.

To finish my acknowledgments, I want to thank all the soldiers and nurses in the frontlines of my beautiful country, knees deep in mud and blood, fighting tooth and nail for every inch of freedom. I salute you, heroes of Ukraine, and I hope to honour your sacrifice someday.

Resumo

Edifícios representam 30% do consumo de energia final a nível mundial, apresentando um grande potencial de redução de consumo energético na luta para a descarbonização da economia. Novas diretivas da União Europeia, com este objetivo em mente, requerem que todos os novos edifícios públicos a partir de 2021 sejam nZEB. Para estudar novas e inovadoras metodologias de atingir essas metas, a UE alocou fundos a projetos inter-nacionais baseados em eficiência energética em edifícios, integração de fontes renováveis e ciência de materiais. O projeto IMPROVEMENT tem como tarefa estudar a integração de fontes renováveis em edifícios públicos, com elevados requisitos de qualidade de potência e conforto térmico, tarefa que juntou vários membros da região SUDOE.

A zona piloto portuguesa faz parte de um laboratório de investigação de uma instituição pública, LNEG, que foi remodelada para uma micro-rede termo-elétrica. Este trabalho foca-se em analisar dados experimentais e criar um modelo numérico em TRNSYS baseados nos mesmos, que possa posteriormente ser usado para analisar melhorias e alterações de equipamento. O sistema de monitorização é apresentado em grande detalhe, junto com todas as renovações que aconteceram no local da área piloto, levando a melhorias significativas no desempenho térmico do invólucro do edifício. Os dados experimentais processados mostram grande promessa de uma micro-rede elétrica funcional, mas são menos positivos no que toca a uma micro-rede térmica sem que haja uma mudança nas estratégias de controlo do sistema. A gestão de energia é crucial para evitar perdas de energia de equipamentos em modo de espera, bem como para minimizar o consumo de energia com uso de monitorização consistente. As mudanças comportamentais dos usuários também são necessárias para operar o sistema em pontos mais otimizados.

Palavras-chave

Nearly Zero Energy Buildings, Eficiência Energética, Indicadores Chave de Performance, Micro-rede, Sistema de Gestão de Energia Elétrica, Sistema de Gestão de Energia Térmica

Abstract

Buildings contain 30% of final energy consumption worldwide, representing a big opportunity in the fight for decarbonization of the economy. New directives from European Union, with this goal in mind, require all new building from 2021 onwards to be near Zero Energy Buildings (nZEB). To study new and innovative methodologies of reaching these goals, the EU has allocated funding to inter-national projects focused on building efficiency, RES integration and material science. IMPROVEMENT project has the task to study the integration of RES systems in public buildings, with high power quality and thermal comfort, which joined together partners from the SUDOE region.

The Portuguese pilot plant is part of a research facility of a public institution, which was retrofitted to a thermal-power microgrid. This work focused on analysing experimental data and creating a numerical model in TRNSYS based on them, which could be used later on to evaluate improvements and changes of equipment. The monitoring system is presented in great detail, along with all the renovations that took place in the pilot area, which improved the thermal performance of the building envelope. The processed experimental data shows great promise of a working power micro-grid, but results are less promising when talking about a thermal micro-grid without a change in the control strategy. Energy management is crucial to avoid energy losses in ”idle” equipment, as well as to minimize energy consumption through consistent monitoring. Behavioural change in users is necessary to operate the system at more optimal points.

Keywords

Nearly Zero Energy Buildings, Energy Efficiency, Key Performance Indicators, Micro-grid, Energy Management System, Thermal Management System

Contents

List of Tables

List of Figures

Chapter 1

Introduction

1.1 Energy consumption in buildings

According to the latest data from IEA, the buildings sector accounts for around 30 $\%$ [1] of final energy consumption and 30 $\%$ for CO_2 emissions. In the European Union and North America, this percentage can be even higher, reaching values of about 40%, which contrasts with the industrial sector percentage in China, which reaches values of almost 60% [2]. The situation in Europe is optimistic, with renewable sources reaching 18.9% of the gross final energy consumption and 30% of total electricity production as well. However, around 60% of the energy consumed is still imported, with the majority being in the form of fossil fuels [3]. This poses a great threat to energy security in EU, which can be balanced out with implementation of more renewables, efficiency measures and new energy policies.

When it comes to the building sector, most of the energy consumed is for space and water heating, totalling approximately 78%. The supply of energy remains mostly in the form of gas, either for space and water heating or cooking, which is a fuel that is mostly imported from countries like Russia. To make use of RES for these uses and decrease the energy intensity of the building sector, new electric devices for the previously specified end uses are being deployed on a commercial scale, which decreases the need to use gas as a primary energy source, creates a much cleaner and efficient energy system with decentralized energy sources [4].

To achieve the goals defined by the Portuguese Roadmap for Carbon Neutrality, the buildings sector also needs energy saving measures to be put in place - passive and active - such as construction of nZEB buildings [5], deep renovations of old buildings, investment in low-emissions energy sources and investigation in low-emissions and environmentally-friendly materials. According to the Decree-Law no. 98/2019 [6], nearly zero energy buildings are - ” Buildings with almost zero energy needs or high energy performance and in which the energy demands can be met with energy from renewable sources, either on site or in the vicinity” Ḃased on this definition, in Portugal new buildings constructed after the year of 2020 are to be designed and built according to these guidelines.

1.2 Objectives and Deliverables

The present work is included in the scope of the ”IMPROVEMENT” project at LNEG - National Laboratory of Energy and Geology - which has a goal of studying solutions for ”Integration of combined cooling, heating and power micro-grids in zero energy public buildings under high power quality and continuity of service requirements”. The scope of this project is related to the INTERREG SUDOE program, which is comprised of several European partners of the SUDOE region (includes the Iberian Peninsula and South-West of France), whose main objective is to facilitate research activities, cooperation and development of the countries that take part in this program.

The work of this thesis will be based on some of the activities included in the WP3 - Work Package 3 - ”*Thermal energy management systems*” - whose main goal is to create and validate a thermal management system for microgrids with renewable production, storage and control. In this work, only the following activities of this specific work package will be presented:

1. Development of a numerical model of LNEG pilot area, thermal renewable production and climatization using TRNSYS software.

2. Validation of the numerical model with experimental data.

3. Extrapolation of the validated model for prolonged periods of time and parametric analysis of several important variables, comparing the results by means of specified $KPIs$.

Due to the large amount of outputs of this project, a selection of more important energy metrics was chosen, which include the seasonal thermal energy savings for different building configurations and the evolution of solar fraction during winter time (which is one of the outputs of the parametric analysis previously mentioned).

The outline of this thesis will reflect some of the stages in building design, which can be seen in the following list:

1. State of the art review: this section will focus on the nZeb methodology by showing examples of nZEB building in Portugal and enumerating different RES integration tecnologies.

2. Description of LNEG pilot plant: brief history of the building, its characteristics, typology and the renovations undertaken in the pilot area.

3. Description of the EMS implemented by SCHNEIDER.

4. Overview of the modelling process: brief description of the whole workflow, from the 3D modelling up to the simulation; indication of the buildings characteristics - materials, gains, occupancy schedules, control strategies for the active systems.

5. Analysis of experimental and numerical results; overview of pilot plant energy production and consumption during the year of 2022; analysis of results obtained from TRNSYS simulation for the proposed configurations.

6. Conclusions: taking into consideration only the metrics for thermal and electric energy, conclusions will be made for the feasibility, or not, of the integration of this type of systems in public buildings.

Chapter 2

State of the Art

2.1 Nearly Zero Energy Buildings

The building sector represents a major opportunity to reduce energy consumption and CO_2 emissions, as it takes around 40% of final energy consumption in Europe. It is imperative to create new policies and formulate innovative strategies for the construction of new buildings, as well as retrofitting and remodelling of older ones, with the goal of minimizing energy consumption, installing local RES and guaranteeing thermal comfort for its occupants.

An nZEB building design is based on the principles of sustainable construction and architecture, which focuses mainly on the following aspects [7]:

1. Shape and orientation of the building.
2. Location of windows and shading devices.
3. Thermal performance of materials.

These measures focus on the passive performance of the building, however these are not enough to reach the nZEB goals of matching consumption with production. For this effect, it is necessary to install local RES to compensate the consumption, which could be in form of solar photovoltaic, solar thermal, wind, geothermal or a hybrid combination of any of the previously mentioned technologies[8].

In Portugal, many examples of nZEB buildings can already be seen, where innovative passive solutions are combined with active systems consisting of RES. One example of this philosophy of sustainable construction is the building SOLAR XXI of LNEG Lumiar Campus. Its design strives to achieve great thermal comfort for the occupants, as well as to push the energy efficiency close to nZeb standards. The shortage of energy production was mitigated with the inclusion of rooftop and wall-mounted photovoltaic panels [9], including a complex energy management system. Passive solutions included installation of shading devices, application of insulation, Trombe walls and design of a ground cooling system, having the sole purpose of reducing thermal energy demand.

Figure 2.1: LNEG Solar XXI building after renovations, South facade [9].

2.2 Integration of RES in buildings

To compensate the consumption of electrical and thermal energy in buildings, it is necessary to install local RES in order to reach the nZEB goals. The type of technology to be installed will depend on the end-use of energy, which can be different from one type of building to another.

Solar energy is the most common source of renewable energy integrated in buildings, with the rooftop installation being the most used method. Other methods have been developed in recent years, such as [10]:

1. BIPV (Building Integrated PV) - Integration of photovoltaic energy in pre-existent components of a building, such as shingles, balcony rails, garage covers. These solutions prove to be an elegant way of integrating solar power into buildings, as they do not require installation of photovoltaic systems, which may not be appealing for the eye, but also removes the need to penetrate the envelope for the fixation of the same systems, which increases the lifespan of the building

2. BIPV/T (Building Integrated PV/thermal - The conversion rate of photovoltaic panels is around 6 to 18%, with the remaining energy left as useful heat. This additional energy can be captured by a cooling circuit fixed behind the panel, such as water or air, and can be used for pre-heating of ventilation air, space/water heating and also to increase the efficiency of said panels.

3. BIPV/L (Building Integrated PV/lighting) - This strategy uses semi-transparent PV films on windows, which capture part of energy as electricity and the rest will be used as natural lighting. It has the advantage of working simultaneously as a shading device, limiting the rise of indoor air by the influence of radiation.

The above mentioned methods work only to produce electrical energy, but many applications in a building also require thermal energy for space and water heating. For these end uses, solar thermal energy is an adequate choice, however, its integration has been more challenging due to the less aesthetic

look of some designs, such as thermo-syphon collector systems, which do not attract engineers and architects to include them in the building planning. Despite this, other models have been developed which hide most of the piping and storage tanks inside the building, with the only setback being the increase of energy consumption as the water needs to be forcefully circulated through the circuit by electric pumps.

Wind energy has not been widely introduced in urban areas, mainly because of the noise and the low wind speed in built environment. However, in recent year new designs have been created, which can prove to be more effective in urban areas than the usual horizontal axis turbines, such as:

1. Radial wind turbines.
2. Vertical axis turbines.
3. Piezo-electric generator.
4. Flag-type triboelectric nanogenerator.
5. Micro-wind turbines.

Despite these recent advancements to include wind energy in urban environments, their efficiency is still very low in relation to conventional horizontal axis turbines, as well as the low technological maturity of many of these modern designs [11].

Another end use in buildings is space cooling, which can be achieved by means of ground source geothermal heat pumps. By using the thermal inertia of the earth, which at several meters underground has a steady temperature of 15 to 18 degrees, the Earth can be used as a massive heat exchanger to cool down water and allow for space cooling even in the hottest days of the year [12]. By combining this technology with solar thermal, it is possible to meet all the thermal energy demands of the building during the entire year.

Other technologies that could prove to be useful revolve around biomass. With this type of energy source, several possibilities arise with the possibility of burning directly biomass to produce heat [13] or to process it in anaerobic digesters and produce bio-gas [14] for cooking and heating applications. However, some of these technologies have a negative impact on the environment and thus are less appealing than the other solutions presented.

Chapter 3

Background

3.1 INTERREG SUDOE IMPROVEMENT: Portuguese pilot area

The pilot area for the study of integration of renewables was chosen to be the Building C of the old IAPMEI Campus. It was built a few decades ago, a time in which regulation on the thermal efficiency of the envelope and integration of active solutions were not as strict as they are today. The old climatization system was composed of outdated HVAC systems and conventional electric heaters, which had an intensive functioning regime due to the high energy demands from the poorly design of the building.

The project begun in 2019, with several European partners from the SUDOE region. This region includes the areas of Portugal, Spain and Southern France, each one dedicated to a specific goal inside of the IMPROVEMENT project. The goal of the LNEG pilot area was to integrate renewable energy systems into public buildings, with the objective of assembling a functioning off-grid system with production, control and storage of energy produced by RES [15]. Apart from the installation of these active systems of energy production and distribution, the pilot area also undergone some structural changes to improve the thermal performance of the envelope:

1. Installation of new ceiling panels with high acoustic and thermal insulation.
2. Installation of a 20cm airbox in the East and West walls.
3. Installation of venetian blinds on East and West windows.
4. Application of a new coating of paint on the walls.

Building C is composed of a ground floor, 1st floor and a basement. On the roof of the building, a small installation exists for housing the old HVAC systems and the most of the components of the IMPROVEMENT project, as well as many arrays of solar collectors, photovoltaics and a small wind turbine. The ground floor concentrates most of the laboratories in the building and some offices, while the 1st floor is occupied mostly by offices and meeting rooms. The basement is used mainly for storage of equipment.

3.2 Location

LNEG has a few campuses spread out in Lisbon and Portugal. The one chosen for the SUDOE IMPROVEMENT is located in Lumiar, in the outskirts of the county of Lisbon, as shown in Figure 3.1a.

Being in the Iberian Peninsula, the campus has available to it plenty of solar resources, with a mean annual irradiation of about 1750 kWh/m^2 [16]. It is an advantage for the implementation of solutions based on solar energy, but it also implies a certain degree of thermal discomfort during the cooling period, which lasts for a large part of the year, as Figure 3.1b shows. The lack of insulation and poor design leads to high energy demand during the cooling season in order to achieve a good degree of thermal comfort.

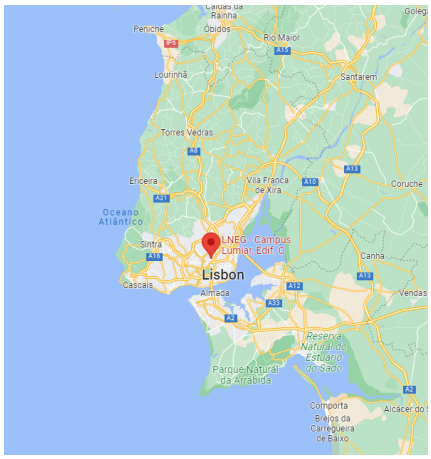

(a) Google Maps location of LNEG Building C.

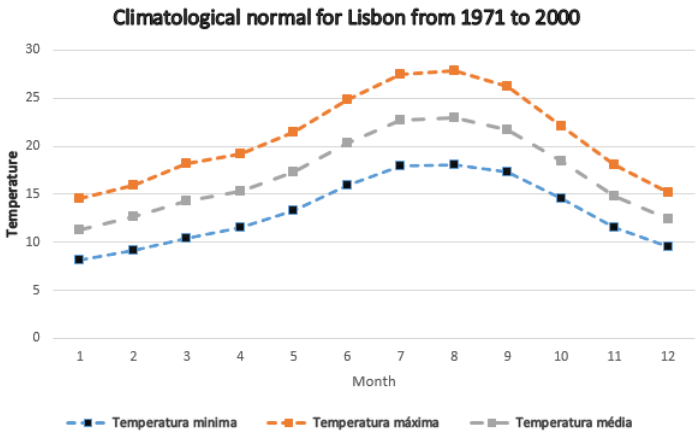

(b) Climatological normal of Lisbon from 1971 to 2000 [17].

Figure 3.1: Location of pilot area (a) and meteorological characteristics of Lisbon (b).

For the numerical analysis, a TMY - Typical Meteorological Year - file was used with data gathered for the Lisbon region. It is a set of meteorological data with data values for every hour in a year for a given geographical location, collected from a period of up to 10 years. The reason why TMY files were chosen is because they already exist in TRNSYS directories and the meteorologial data that they output are tuned in for the software itself - data gathered on site at LNEG only measures certain quantities, so for some specific parameters it requires the use of models or extrapolations to have an estimate of the values needed. For the validation of the numerical model, the meteorological data used came from a station at LNEG campus as it represents more clearly the real-time meteorological conditions on-site.

3.3 Geometry of pilot area

As previously mentioned, the pilot area only includes a small area of the building, on the ground floor in the South-West corner. Image 3.2 shows the top view plan of the ground floor, with the pilot area selected in orange.

In Table 3.1, each individual space of the pilot area is described in terms of its real area and volumes, which are necessary as an input to the numerical model further on.

Figure 3.2: Top-view of the cross-section of the ground floor of Building C of LNEG Campus in Lumiar; highlight in orange corresponds to the pilot plant area.

Room	Functionality	Area (m^2)	Volume (m^3)
1052	Conference room	83.4	225.29
1054	Meeting room	22.1	66.27
1050	Office	10.8	32.43
1051	Office	10.8	32.43

Table 3.1: Areas and volumes of monitored pilot plant rooms.

3.4 Energy and Thermal Management System

To gather data and monitor the proper operation of all the thermal and electrical equipment, an Energy and Thermal Management System (ETMS) was put in place before and after the renovations. These systems are composed of the proper sensors and power tags to gather data on temperature, CO_2 levels, humidity and power, giving a real-time visualization of the comfort levels in the pilot area, state of the electric grid and of the thermal system.

After the renovation of the pilot area, a more advanced system was designed by the LNEG team and the installation was outsourced to a team from SCHNEIDER. A graphic interface was created, which can supply a real-time graphic visualization of the state of electric and thermal systems, as well as the balance of energy produced by PV, energy consumed by the pilot area and the energy supplied to the grid. Besides data gathering, it also has a connection to the SCADA control system which allows it to change setpoint temperature, modes of operation and shut down some of the loads.

3.4.1 Pre renovation EMS

Before renovations, this system focused mainly on gathering data from the Room 1052, such as air temperature of rooms, surface temperatures, humidity and CO_2 levels, which was useful to create a preliminary thermal model of the space and design of the climatization system, as well as to pinpoint critical areas for any structural changes.

According to Figure 3.3, the sensors in red are thermocouples, which were connected to a data-logger and only measured temperature according to the place they were placed on. The data collection from the logger occurred every 10 minutes. This implied a regular flush of data from the logger, which if not done properly and on time, would overwrite the existent data with newly collected information and ruin the dataset.

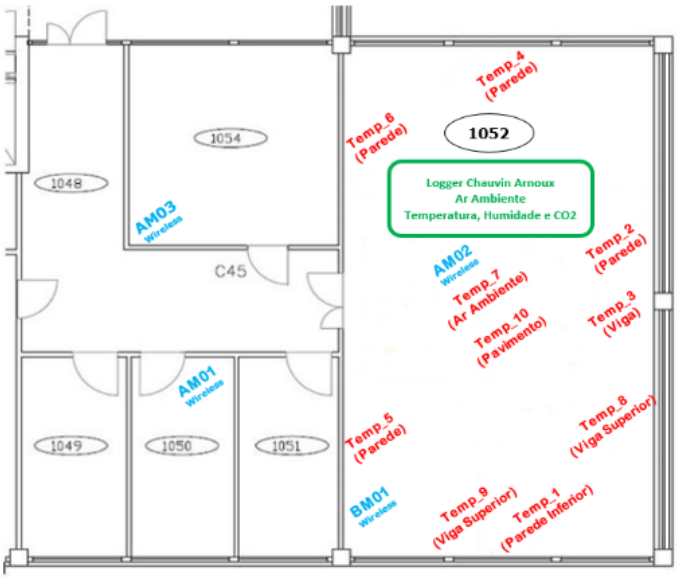

Figure 3.3: Location of sensors in the pilot area before renovations.

The sensors in blue are wireless, which were connected to a cloud server and measured temperature, CO_2 levels and humidity, with one special sensor installed to monitor light intensity. The data was recorded at irregular intervals, which made challenging the treatment of data, and the wireless configuration implied that batteries had to be changed regularly when the levels of charge would become too low. In Table 3.2, a list of the sensors installed previous to the renovations is shown along with the main purpose of each of these sensors.

Due to the irregular nature of data supplied for the monitored rooms 1054, 1050 and 1048, the validation of results pre-renovation will be conducted only for the room 1052, as the data from the thermocouples is more reliable and regular in time.

Sensor	Measurement	Sensor	Measurement
Temp 1	Lower W wall temperature	Temp 2	S wall temperature
Temp 3	Middle pilar of S wall temperature	Temp 4	Lower E wall temperature
Temp 5	Room 1051 adjacent wall temperature	Temp 6	Room 1054 adjacent wall temperature
Temp 7	Ambient temperature	Temp 8	S wall top beam temperature
Temp 9	W wall top beam	Temp 10	Ground floor temperature
AM01	Temperature, humidity and CO_2 of room 1050	AM02	Temperature, humidity and CO_2 of room 1052
AM03	Temperature, humidity and CO_2 of room 1054	BM01	Temperature, humidity, CO_2, light intensity and particulate matter of room 1052

Table 3.2: Sensors installed pre-renovations and their function.

3.4.2 Post renovation EMS/TMS

The sensors installed after the renovations allowed the creation of an online monitoring platform, which showed real-time data of the electric and thermal systems, as well as comfort levels in the monitored areas. It also allowed for easy access to collected data in any place and time, as long as the user was connected to the platform.

Comfort

Figure 3.4 shows the placement of sensors that measure comfort parameters. Apart from the comfort parameters being measured, it also shows the power consumed by the pilot area, such as lightning and equipment.

The following list sums up all the parameters that are being monitored in each of the areas:

1. Room 1048 - air temperature, humidity, CO2.
2. Room 1050 - air temperature, humidity, CO2.

3. Room 1052 - air temperature, humidity, CO2, surface temperature, light intensity.

4. Room 1054 - air temperature, humidity, CO2, surface temperature.

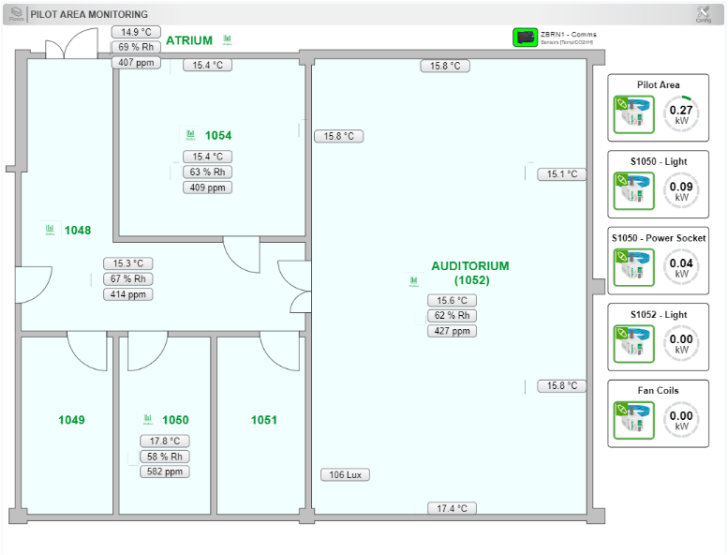

Figure 3.4: Comfort monitoring window from SCHNEIDER online platform.

Electrical system

In Figure 3.5 is shown a real-time visualization of consumption vs production in the pilot area. The production is separated into two components:

1. Solar - I, V, P, E and frequency (P and E are divided into the three components - active, reactive and apparent).

2. Wind - same parameters as solar.

The consumption variable is divided into different power-tags spread around several pieces of equipment of the pilot area, each one measuring specific electric parameters.

1. Fan coils (total) - I, V, pf, P_{active} and E_{active}.

2. Lightning room 1052/1050 - I, V, pf, P_{active} and E_{active}.

3. Power socket 1050 - I, V, pf, P_{active} and E_{active}.

4. Heat pump - I, V, pf, P_{active} and E_{active} (I and V measured for the three phases that this equipment operates on).

The scheme of the electric system includes three different inverters: one for solar, one for wind and one to manage the input/output of energy from and to the grid. It receives the energy produced by solar/wind and delivers it to the grid, while pulling from the grid the energy needed to supply the pilot area with the required amount of electricity. Although the SOC of batteries has not been monitored due to technical issues, a few temperature sensors were installed for safety measures.

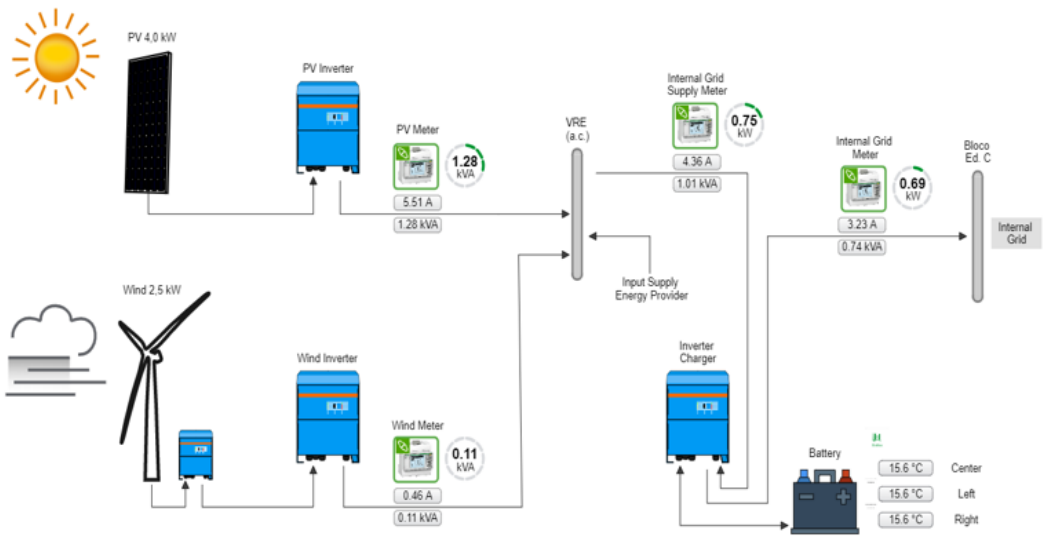

Figure 3.5: Electric monitoring window from SCHNEIDER online platform.

Thermal

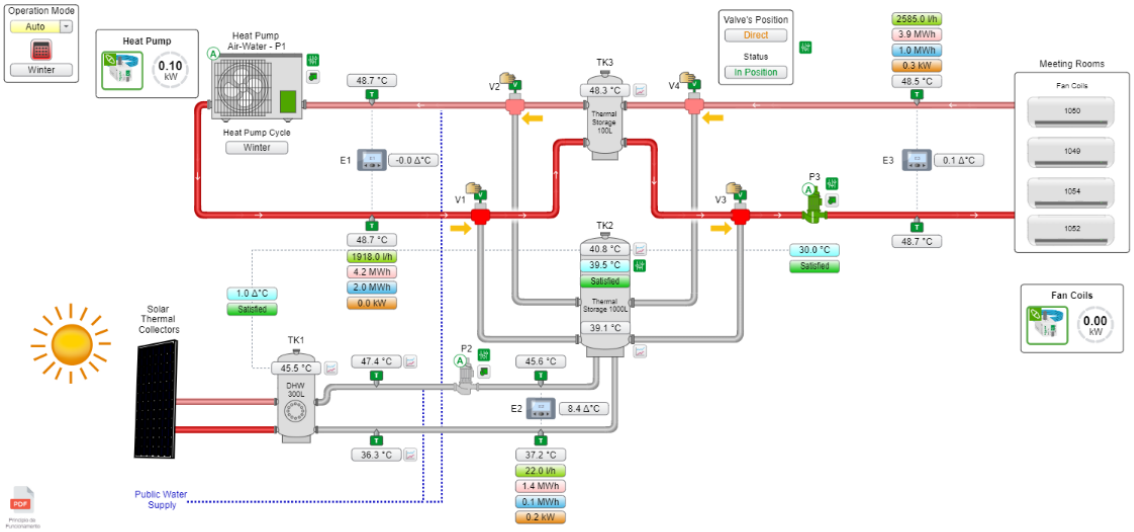

Figure 3.6: Thermal monitoring window from SCHNEIDER online platform.

For the thermal installation of the LNEG pilot plant, three different sub-systems can be defined, being all connected to a central storage tank (TK2) of 1000L, model LAPESA G-1000 IIS.

Three different enthalpy sensors are installed, each measuring the flowrate and temperature difference to calculate the energy delivered or consumed according to whether the system is in cooling or heating and the location of the sensor.

1. E1 - enthalpy meter that measures the energy delivered to the pilot area through the climatization system.

2. E2 - enthalpy meter that measures the energy delivered to the TK2 from the solar tank (TK1) when

in economic mode; if the system is in direct mode, this becomes irrelevant and is only useful to verify leakage flow from TK1 to TK2 due to pressure build up.

3. E3 - enthalpy meter that measures the energy delivered by the heat pump; when in economic mode, it measures the energy delivered to TK2, while in direct mode it measures the energy supplied to TK3.

The heat pump and fan coils consumption are also presented, but these values are only useful for the balance of the electric system and for pure monitoring of proper functioning of the thermal equipment.

3.4.3 Thermal Energy Management System

The thermal system can be operated in two different modes: economic and direct. In economic mode, the goal is to maintain the setpoint temperature of TK2 at a specified level, with the assistance of the heat pump and of the solar collectors (only during heating season). The direct mode connects directly the fan-coils circuit to the heat pump, bypassing the large storage tank and going through the smaller 100L water tank (TK3). Despite these differences, the circulation of the water in the fan-coils circuit is done by the same pump, P3, which is activated at all times.

The change between both of these modes of operation was done manually to verify differences in performance and energy efficiency between them.

Direct mode

Apart from the economic configuration, the system has a direct configuration, which connects the heat pump directly to the fan-coils, similar to how a normal HVAC system works.

Depending on the season, the temperature of the smaller storage tank has to be at a certain level, since the fan-coils require a temperature differential high enough to work efficiently.

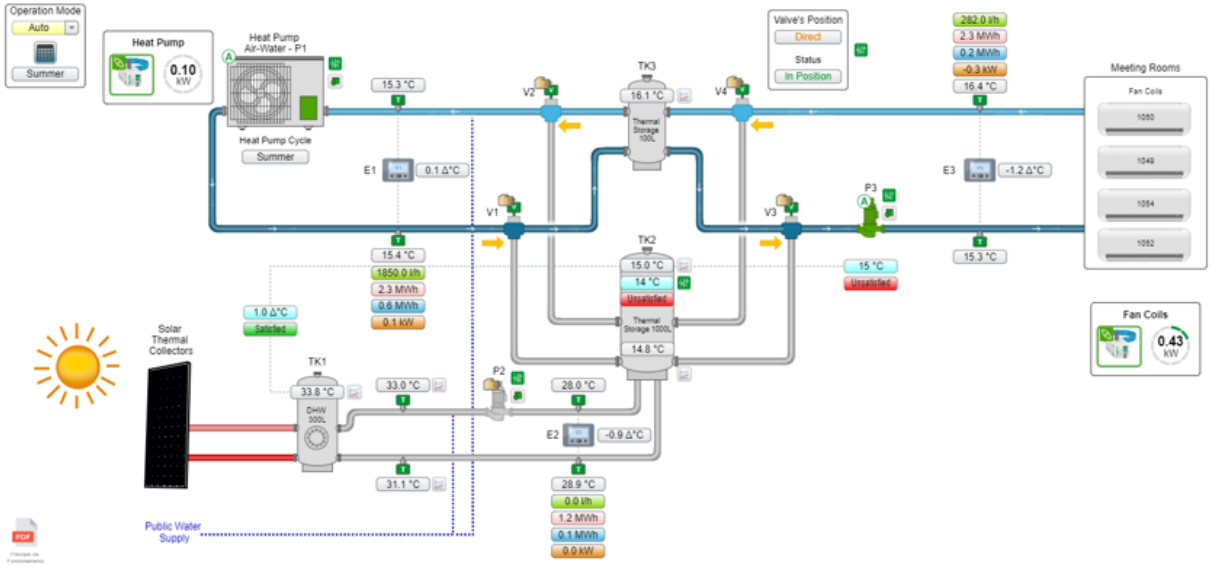

Figure 3.7: Capture of the TMS from Schneider during cooling season in direct mode.

Economic mode of operation

For this operation mode, the heat pump and solar sub-systems work only to maintain a specified setpoint temperature in the 1000L storage tank.

Lisbon´s geological location is prone to longer cooling seasons in contrast to heating seasons, but it is rather impossible to precisely define the length of these periods because of extreme weather fluctuation in past years. For the purpose of this project, the heating season was defined from 1st of November up to 31st of March, which coincides with the months of maximum air temperatures below 20ºC according to Figure 3.1b.

In any case, if meteorological predictions point to lower/higher temperatures in contrast to the usual pattern, the system can be turned on manually from heating to cooling, according to the needs of the building.

During the heating period, which was defined from the 1st of November to 31st of March, the pump P2, which connects the solar sub-system to the central tank, can be turned on when:

1. The temperature of the solar tank TK1 is superior to the temperature of mixture tank TK2.

2. The temperature TK2 has not reached the setpoint temperature.

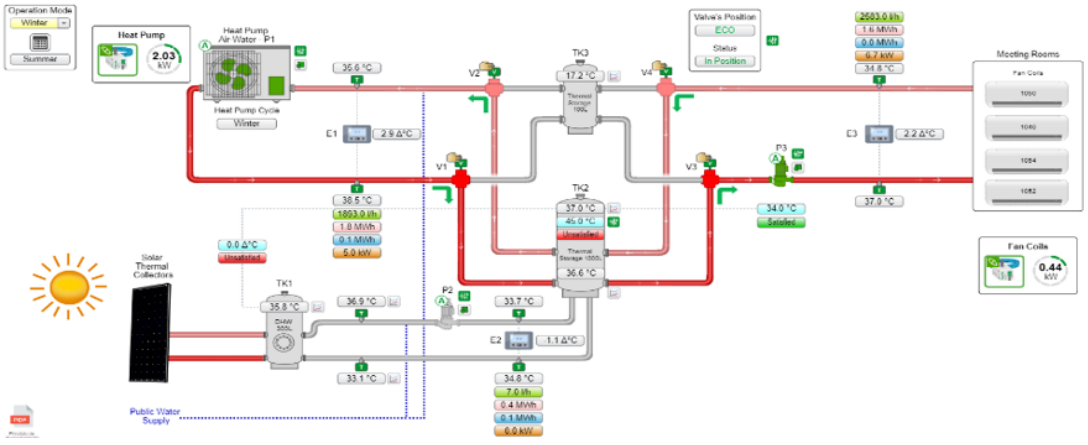

Figure 3.8: Capture of the TMS from Schneider during heating season in eco mode.

The heat pump and the corresponding circulation pump P1 is activated only when:

1. The temperature of the mixture tank TK2 is lower that the setpoint and the solar system is not active.

2. The solar system is active, however the energy supplied by it is not enough and the temperature of the mixture tank decreases as a result.

During the cooling period, the solar system is disconnected from the rest, as the solar thermal energy is not useful for cooling needs. All the energy needs are supplied by the heat pump, whose only objective is to turn on when the setpoint temperature of the mixture tank is not met.

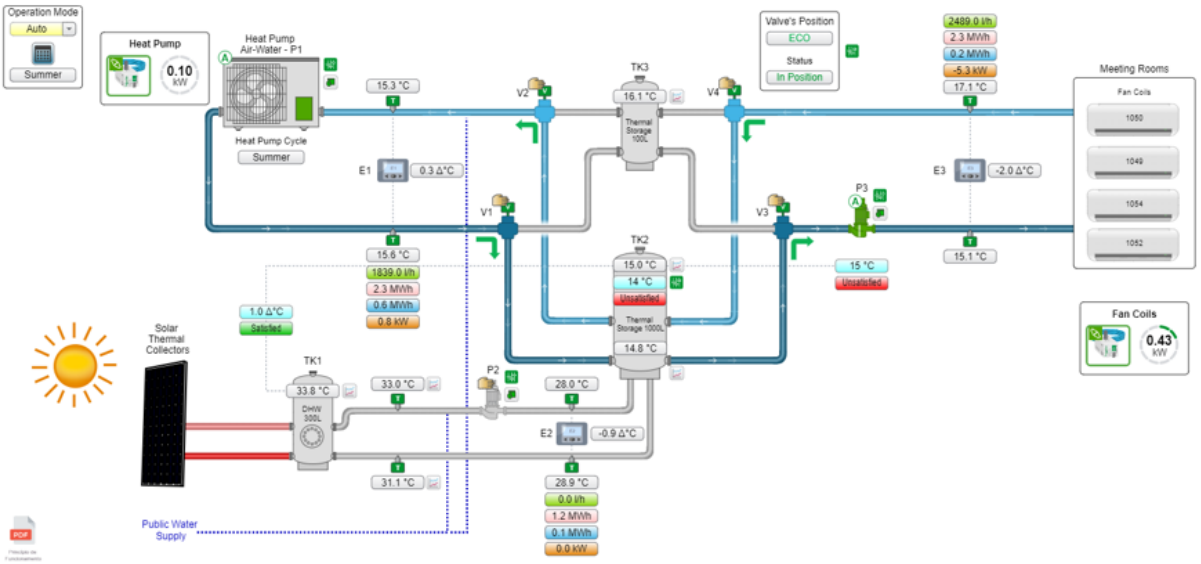

Figure 3.9: Capture of the TMS from Schneider during cooling season in eco mode.

3.5 Overview of monitoring system

1. Comfort:
   (a) Room 1048 - air temperature, humidity, CO2.
   (b) Room 1050 - air temperature, humidity, CO2.
   (c) Room 1052 - air temperature, humidity, CO2, surface temperature, light intensity.
   (d) Room 1054 - air temperature, humidity, CO2, surface temperature.
2. Electrical:
   (a) PowerTag - Fan coils, Heat Pump, Room 1050/1052 Lightning, Room 1050 Power socket.
   (b) PV Energy Production.
   (c) Total supply by Public Grid.
   (d) Total supply to Microgrid.
   (e) Wind Energy Production.
3. Thermal:
   (a) Entalpy meters E1, E2, E3.
   (b) TK1, TK2 and TK3 temperatures (TK2 Down Temperature - T4, TK2 Up Temperature - T3).

3.6 Bill of Equipment

In Table 3.3, a list of the equipment is shown, organised by each sub-system. Some of the equipment was repurposed from older projects, as is the example of the inertial tank, and some was offered by companies willing to spread awareness for their products, like the case of the solar collectors.

As no technical data-sheets were found for the circulation pumps, no models are presented here. However, since the enthalpy meters supply information on the flowrate for each of them, it was only necessary to find generic circulation pumps with the same flowrate and take the power consumption to input in the numerical model.

Subsystem	Component	Model
Solar	Evacuated tube collector	BAXI AR30 [18]
	Solar tank	BAXI FST 300L [19]
	Primary circulation pump	
	Secondary circulation pump	
Heat pump	Air-to-Water heat pump	DAITSU CRAD 2 60T [20]
Climatization	Room 1052 fan-coil	FDLA AC TS 54 [20]
	Room 1054 fan-coil	FMCD EC TOTAL 20 [20]
	Room 1050/1051 fan-coils	FMCD EC TOTAL 06 [20]
	Circulation pump	
Air renovation	Heat exchanger unit	HRD EC 1000 [20]
Thermal storage	Inertial tank	LAPESA G1000 IS-02 [21]
	Small tank for direct mode	BAXI 100L [19]

Table 3.3: Bill of Materials for the installation of the LNEG pilot area.

Chapter 4

Numerical model

$TRNSYS$ is a flexible and complex software tool, made by TESS - Thermal Energy System Specialists - used specifically for the simulation of transient systems. It is useful not only to simulate the active components, such as solar collectors, photovoltaic panels, electric grids, climatization systems, but it is also useful for the study of the passive part of any building, with multiple zones or not [22]. Although this software can be more complicated to operate compared to other tools, such as *Modelica* [23], it has a much faster computation time and the user supplied functions, or Types as they are called in TRNSYS, enrich the software with various tools to solve complex dynamic systems.

As the LNEG pilot area makes use of a lot of thermal equipment - heat pump, solar collector, fan coils - it was of high importance to use TRNSYS to understand the thermal behaviour of the building, as well as the contribution of the solar collectors for the climatization of the used space.

4.1 3D modelling - SketchUp

The first step is to create a geometrical model of the building in a 3D modelling tool called SKETCHUP. Geometrical data can only be imported to TRNSYS from this software, as it allows for the creation of thermal air nodes and shading groups.

Each thermal air node represents a room, which is modelled individually in the next steps of the process. Each surface needs to be defined with the correct adjacencies to the surrounding air nodes, as it is important to know whether it is an internal or external wall, floor, ceiling and ground floor due to the boundary conditions that each one of these definitions imply. For this reason, the 3D model of the pilot area also includes the top floor right above it and an additional part of the building to the side.

The shading groups represent all the elements that can create shade on the building, which can include trees, other buildings, and other physical elements.

Although some trees exist adjacent to the South wall, a simplification was made to not include them due to their small size and overall coverage.

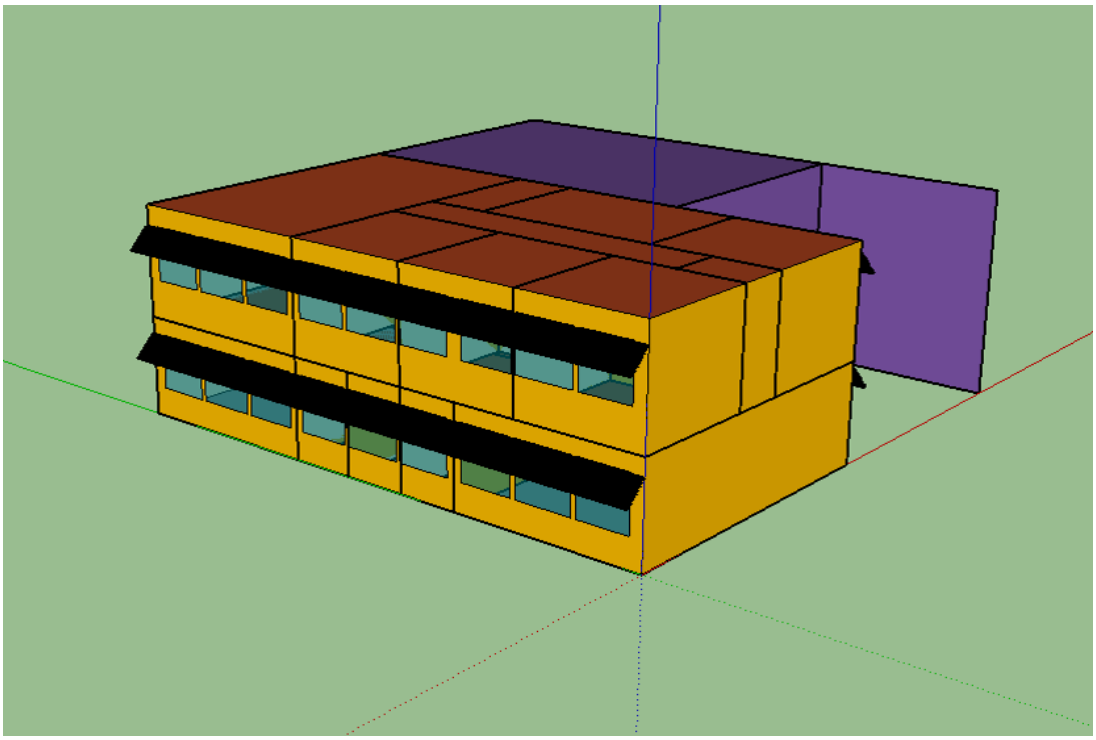

Figure 4.1: 3D Model of pilot area and near vicinity, including shading surfaces (in purple).

4.2 Building modelling - TRNBUILD

To create a TRNSYS project with the geometry that was presented previously, Type 56 must be used, which connects to a pre-installed plug-in called TRNBUILD [24]. This plug-in was made specifically for modelling of multi-zone buildings and it is essential in the elaboration of the numerical model of the pilot area, as it is composed of several separate zones.

This building modelling environment comes with the ability to assign materials, occupancy schedules, internal gains and even daylight controls. Some of the options require specific inputs from the simulation environment, such as ventilation, but it also has the ability to export outputs into the same environment. This interchange of inputs/outputs between both environments is mandatory to accurately model the interaction between the active systems and the thermal response of the building to meteorological conditions/occupancy.

In the following sections, a brief explanation is given for each step in the modelling of the pilot area in TRNBUILD, based on software documentation [25].

4.2.1 Wall layers

In Table 4.1, the current composition of the wall materials is presented. It must be pointed out that this configuration is different from the one before renovations began, as some of the walls have different compositions due to the structural changes that the pilot area went through.

Layer	Material	Thickness (m)	Heat loss coefficient $U(W/m^2C)$
Ground floor	Ceramic tile	0.02	0.208
	Lime and cement mortar	0.002	
	Concrete slab	0.15	
	Insulation*	0.15	
Interior wall	MDF	0.008	0.614
	Rockwool	0.05	
	MDF	0.008	
Middle floor	Ceramic tile	0.02	0.540
	Lime and cement mortar	0.002	
	Concrete slab	0.15	
	Air	0.15	
	Plaster board with anti-humidity and sound insulation	0.025	
Roof	Ceramic tile	0.02	0.426
	Polyurethane insulation	0.04	
	Concrete slab	0.15	
	Air	0.15	
	Plaster board	0.025	
South and North walls	Ceramic tile	0.005	0.526
	Lime and cement mortar	0.002	
	Hollow clinker	0.18	
	Air	0.05	
	Hollow clinker	0.18	
East and West walls	MDF	0.008	0.407
	Rock wool	0.05	
	MDF	0.008	
	Air	0.2	
	MDF	0.008	

Table 4.1: Description of layers from each modelled wall and respective global heat loss coefficients.

4.2.2 Windows

	Material	Thickness (mm)	Distance between layers (mm)	Heat loss coefficient $U(W/m^2C)$
Real window	Glass	6	13	2.68
TRNSYS model ID 601	Glass	5.7	12.7	2.85

Table 4.2: Material properties between real-life windows model and TRNSYS.

The window model is a typical double glass layer, with a distance of 13mm between them. Although TRNSYS already includes many different windows in its libraries, there were no identical models with the one used in the pilot area. So a window was chosen, with similar thickness and spacing, which results in a slightly different loss coefficient, as can be seen in Table 4.2.

4.2.3 Infiltration

After defining the wall layers and windows, the next step is to define the infiltration rate in the building. As no tests were performed in each individual area of the pilot plant, a general infiltration rate was defined as per rules of ASHRAE HOF Chapter 16. This information was taken from the extensive tutorials supplied by the software package.

According to this definition, a typical building has an infiltration rate of $5.4m^3/h\ m^2$ per external wall area - multiplying by the external area of the geometrical model and dividing by the total volume, an approximate value of 0.6 ARH was calculated. This definition is related to older buildings, in which the infiltration rates tend to be higher - however, this does not take into consideration wind speed, temperature and pressure difference between the interior and exterior, among other factors. For future investigations, it is advisable to conduct proper tests in order to determine a more accurate value for this variable.

4.2.4 Internal gains

Three different internal gains can be defined for each of the areas of the pilot plant. In TRNBUILD, there must be a clear division between convective and radiative gains that each of these types emit, because of the way how TRNSYS calculates energy balances inside of an air node.

1. People - Depending on intensity of physical activity and type of clothing, the gain from existence of people inside of any air node can change, as well as the percentage between convective and radiative gains. The basis for this model was the $EN13779\ 125W\dot{2}4^oC$ norm, which fixes the gains for an Activity of Level 3, describing sedentary activity in an office with formal attire. This information was taken from existent TRNSYS libraries.

2. Lighting - Since the type of lighting used in the renovated space was chosen to be LED lights, the majority of the gain come from the radiative part (40 $\%$) while the rest comes in terms of convective gains. The power rating of the lights is about $58W$.

3. Equipment - Per default, as suggested in TRNSYS documentation, an equal division between radiative and convective gains was defined. The power rating for the equipment, which consists mostly of personal computers, was fixed at $50W$.

Each of the areas inside of the pilot plant has a specific occupancy schedule, which will influence the overall energy demand and create periodic peaks when the whole pilot area is at full capacity. The occupancy schedule will determine the activation of all the gains, so as when a ”person” enters the building, all the lights and equipment are turned on and remain constant through the occupancy schedule.

Gain	Convective (W)	Radiative (W)
People	37.5	37.5
Lightning	23.2	34.8
Equipment	25	25

Table 4.3: Summary of internal gains defined for pilot area.

For the validation of results, these schedules were adjusted to correspond to the real occupancy during the time period chosen for validation - this is an important feature of a public building as LNEG, since occupancy schedules can vary throughout the year. As a simplification, they remain constant through the year, without counting holidays.

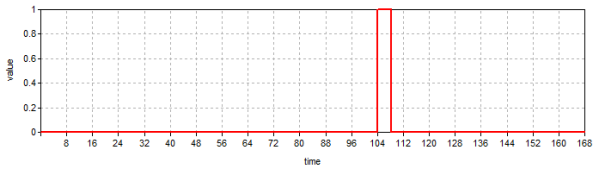

(a) Weekly schedule for Room 1052.

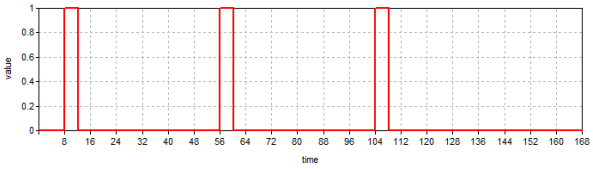

(b) Weekly schedule for Room 1054.

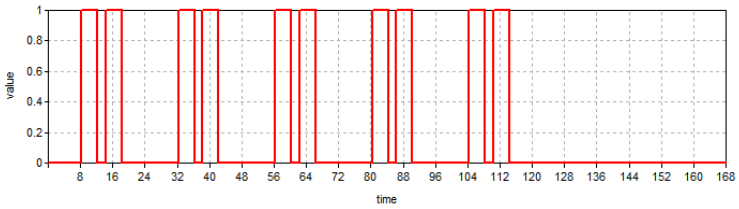

(c) Weekly schedule for Rooms 1050/1051.

Figure 4.2: Weekly schedules for monitored areas.

For the offices, every day occupancy is expected, with an usual working schedule from 8:30 AM to 12:30 PM and from 14:30 PM to 18:30 PM. For the Room 1054, the occupancy is expected to be much lower, as this area is only used for small staff meeting, so Monday, Wednesday and Friday it is occupied from 8:30AM until 12:30 PM. As for the Room 1052, it is only expected to have one big meeting every week on Fridays, with the same occupancy period as the Room 1054.

TRNBUILD has an option where these schedules can be defined inside of the building modelling environment, however they are used as inputs from the simulation environment, where the exact same schedules can be created for daily, weekly and monthly time scales.

4.2.5 Lightning control

The pilot area has a dimmable switch for lightning control, however inside the simulation environment its control is based on the ”on-off” principle since the installation does not have an automatic control over the dimming. Due to this reason, the lights will remain always at the highest intensity, which will result in a slight overestimation of internal gains.

4.2.6 Ventilation

To simulate the operation of the fan-coils inside of the pilot area, a ventilation type must be assigned to each of the air nodes where it is installed. It will work in a tight interaction with a model of the fan coils in the Simulation Studio, each using the outputs of the other as inputs.

Figure 4.3 shows the principle of modelling a ventilation system in TRNSYS. The important variables in each of the ventilated areas are the air temperature (C), relative humidity ($\%$) and mass flow (kg/hr). One model exists in the TRNBUILD environment and one in the Simulation Studio environment - as the air circulates, the inputs from one model work as outputs for the other during the specified operation of the fan-coils, which are defined in the Simulation Studio.

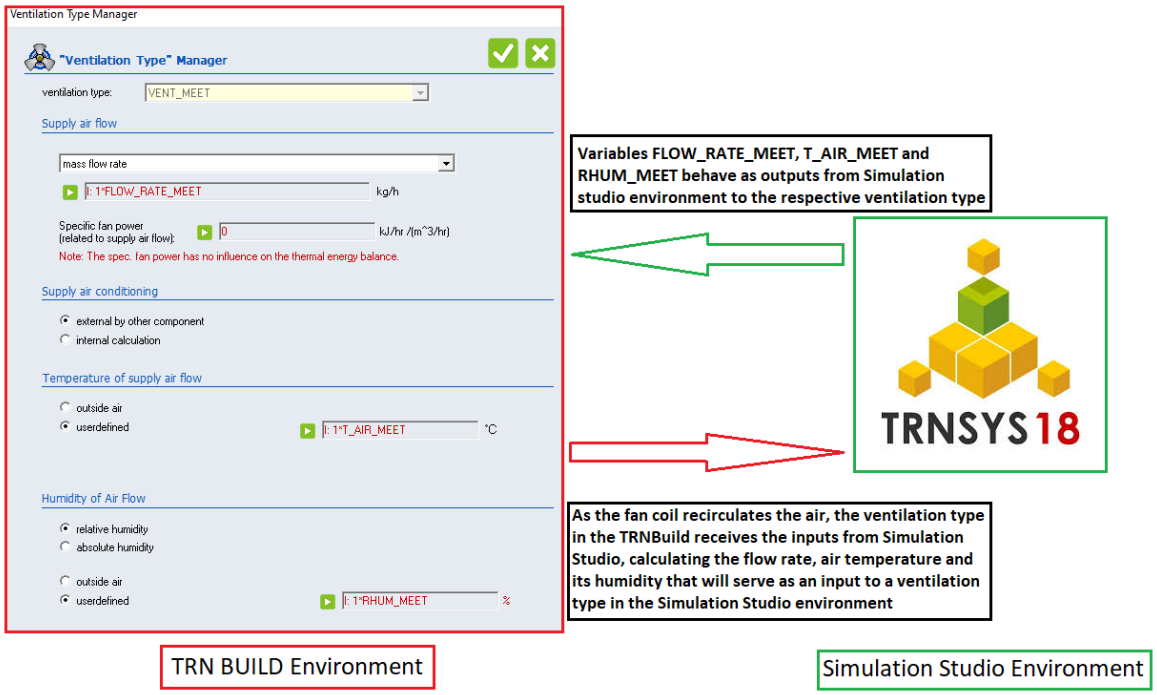

Figure 4.3: Scheme of working principle of the ventilation system.

4.2.7 Physical properties

To end the building model, it is necessary to add some physical properties, which are important in the energy balances of TRNSYS.

First of all, it is important to properly define the radiation on the building´s surfaces by taking into consideration the inclination it has from South to East.

By finding the turn angle in Figure 4.4, the radiation on the North, East, West, South and horizontal surfaces was corrected by the use of Type 16, which takes into consideration the horizontal radiation and azimuth of the surface, computing the beam and diffuse radiations on each of directions, as well as the incidence angle.

Following up, it is also recommended to change the air and humidity capacity for each of the spaces.

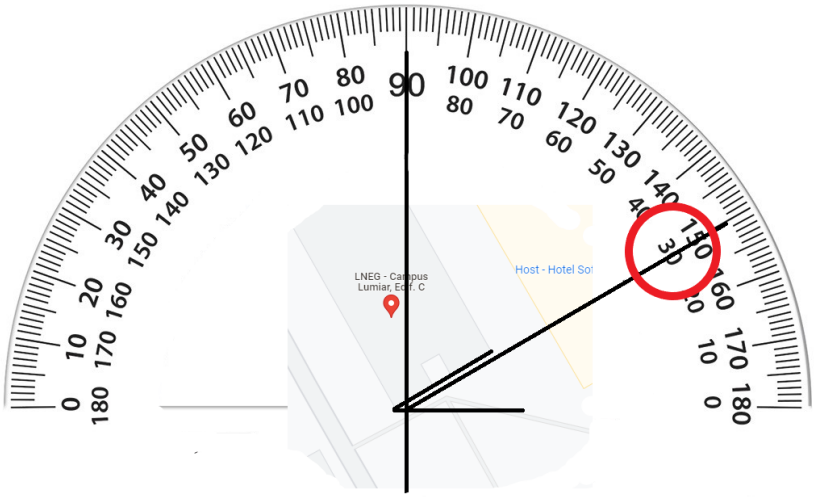

Figure 4.4: Turn angle of LNEG building.

The air capacity is a fixed value, which exemplifies the ability of dry air to absorb energy - however, for an office space with a lot of furniture such as LNEG, it is necessary to multiply the common value of air capacity by 5 to 10 times in order to account for all the extra materials capacity as well.

Moisture capacity is the ability of moisture in the air to absorb energy. The ”Simplified Humidity Model” was used, which the humidity capacitance ratio was fixed at 10 for each space.

4.3 Climatization modelling - TRNSYS Simulation Studio

To define any physical phenomenon, create occupancy schedules or simulate the operation of many different electric and thermal equipment, the user has available to him an extensive list of pre-defined functions which are called ”Types”. Although it is possible to create new types, for this work only types in existing TRNSYS libraries were used.

In Table 4.4 are represented the types related to the equipment listed in the table. Although other types were used, they only act as control, output and scheduling functions, which can be considered to be supporting elements to the numerical model.

To simulate the operation of the pilot area equipment, the following schedules were defined for each of the subsystems:

1. Heat pump - Monday to Friday, from 8:00 to 20:00.
2. Fan coil circulation pump - Monday to Friday, from 8:00 to 20:00.
3. Renovation circuit - Monday to Friday, from 9:00 to 12:00 and from 13:00 to 18:00.
4. Solar system - Monday to Sunday, from 10:00 to 17:00.

Subsystem	Component	TRNSYS Type
Solar	Primary pump	Type 114 - Single speed pump
	Secondary pump	Type 114 - Single speed pump
	Solar tank	Type 156 - Cylindrical Storage Tank with immersed heat exchanger
Heat pump	Heat pump	Type 941 - Air-to-Water Heat Pump
	Circulation pump (internal)	Type 114 - Single speed pump
Climatization	Fan coils	Type 600 - 2-Pipe Fan coil (adjusted for each model)
	Circulation pump	Type 114 - Single speed pump
Air renovation	Heat exchanger	Type 760 - Sensible Air-to-Air Heat Recovery with Controlled Outlet Conditions
	Fans	Type 146 - Single speed fan

Table 4.4: List of key components of LNEG pilot area thermal system and the TRNSYS counterparts.

4.3.1 Control

Each of the equipment has a unique controller, however the access to their technical specifications is denied by their respective manufacturers. For this reason, the control strategies will be based on "On-Off" controller dependent on certain temperatures.

Solar circuit

The solar circuit has two components that have to be controlled: the primary and secondary circulation pumps. As they are only required to work during the heating period, they have no control strategy for the cooling season as they are shut off during that time.

The primary pump control reads the values of temperature from the outlet of the solar collector - T_{out}^{coll} - and from the middle of the solar tank - T_{solar} (where a sensor is located near the heat exchanger outlet). As for the secondary pump, it needs the values of temperature from the outlet of the solar tank - T_{solar}^{out} - as well as from the middle of the inertial tank - $T_{inertia}$.

The following logical equations represent the control strategy for both these pumps - when true, they activate the equipment and when not it is turned off.

$$T_{out}^{coll} - T_{solar} > 1 \wedge T_{solar} < 80 \tag{4.1}$$

$$T_{solar}^{out} - T_{inertia} > 1 \wedge T_{inertia}^{out} < T_{inertia}^{setpoint} \tag{4.2}$$

For the primary pump, two conditions must be met: the water coming out of the collector must be at least $1°C$ hotter than the water at sensor height in the solar tank, while it also prevents the pump from activating when the same sensor reads values of temperature superior to $80°C$.

For the secondary pump, the water coming out from the solar collector must be superior by $1°C$ to the water at sensor height in the inertial tank, which only works up until the water at the outlet of the inertial tank remain below the designated setpoint temperature.

Heat pump

The heat pump is composed of two components which are to be controlled by the same control action. As the heat pump works during the heating and cooling season, two different control strategies must be created for each of these time periods.

$$T_{out}^{inertia} < T_{setpoint}^{heating} - 1 \tag{4.3}$$

$$T_{out}^{inertia} > T_{setpoint}^{cooling} + 1 \tag{4.4}$$

$$C_{pump} = C_{hp}^{heating} + C_{hp}^{cooling} \tag{4.5}$$

Equations 4.3 and 4.4 represents the moment at which the heat pump is enabled (heating and cooling period respectively), while the control for the circulation pump is represented by equation 4.5 - it activates whether the system is in cooling or heating mode ($C_{hp}^{heating}$ and $C_{hp}^{cooling}$ are the representative logical variables for the heating and cooling control of the heat pump). The heat pump then has an additional control, which prevents it from going over the setpoint temperature (during heating season) or under (during cooling).

Fan-coils

Due to a more detailed technical information supplied by the manufacturer´s, it was possible to obtain a more precise control strategy for the ventilation system. The fan-coils operate in cooling and heating mode and do so according to the difference between the actual room temperature and the room setpoint temperature.

The fan coils have 2 modes of operation: automatic and manual. The manual mode consists of manually choosing the fan speed in the controller, which will supply a constant air-flow with no regards to the change in room temperature up until the setpoint is met. The automatic mode consists of a control strategy that changes the air-flow according to the room temperature.

Automatic mode consists of three speeds: high (H), medium (M) and low (L). Each of the fan-coil models used has a different set of speeds, but the control strategy remains the same for all. Apart from the air-flow, other variables are also regulated by this same logic: water flow and coil pressure drop. It is important to note that the control of this subsystem is done every 15 seconds and the control strategies presented further only take into consideration the current temperature reading and the last one.

During the heating season, the fan coils are activated when the air temperature is below the setpoint. Two situations can occur for the room temperature: it can wither be going up or down. Following are the equations that represent the control strategy implemented for the heating.

$$
\begin{aligned}
&if\ T_{air}^{i} - T_{air}^{i+1} < 0\ \wedge \Delta T = T_{air} - T_{setpoint} \\
&FC_{speed} = H \longleftrightarrow if\ \Delta T < -3 \\
&FC_{speed} = M \longleftrightarrow if\ \Delta T < -2\ \wedge\ \Delta T > -3 \\
&FC_{speed} = L \longleftrightarrow if\ \Delta T < -1\ \wedge\ \Delta T > -2
\end{aligned}
\tag{4.6}
$$

$$
\begin{aligned}
&if\ T_{air}^{i} - T_{air}^{i+1} > 0\ \wedge \Delta T = T_{air} - T_{setpoint} \\
&FC_{speed} = H \longleftrightarrow if\ \Delta T > -3\ \wedge \Delta T < -2 \\
&FC_{speed} = M \longleftrightarrow if\ \Delta T > -2\ \wedge\ \Delta T < -1 \\
&FC_{speed} = L \longleftrightarrow if\ \Delta T > -1\ \wedge \Delta T < 0
\end{aligned}
\tag{4.7}
$$

As for the cooling period, the fan coils are activated when the air temperature is above the setpoint temperature. Because of this, the strategy for the cooling period control follows an inverse logic compared to the heating period.

$$
\begin{aligned}
&if\ T_{air}^{i} - T_{air}^{i+1} > 0\ \wedge \Delta T = T_{air} - T_{setpoint} \\
&FC_{speed} = H \longleftrightarrow if\ \Delta T > 3 \\
&FC_{speed} = M \longleftrightarrow if\ \Delta T > 2\ \wedge\ \Delta T < 3 \\
&FC_{speed} = L \longleftrightarrow if\ \Delta T > 1\ \wedge\ \Delta T < 2
\end{aligned}
\tag{4.8}
$$

$$
\begin{aligned}
&if\ T_{air}^{i} - T_{air}^{i+1} < 0\ \wedge \Delta T = T_{air} - T_{setpoint} \\
&FC_{speed} = H \longleftrightarrow if\ \Delta T > 2\ \wedge \Delta T < -2 \\
&FC_{speed} = M \longleftrightarrow if\ \Delta T > 1\ \wedge\ \Delta T < 2 \\
&FC_{speed} = L \longleftrightarrow if\ \Delta T > 0\ \wedge \Delta T < 1
\end{aligned}
\tag{4.9}
$$

The same way as the airflow is controlled according to these strategies, the water flow though the coils and the respective pressure drop is also modelled in the same manner.

4.4 Verification and Validation

To extract meaningful data from the simulation environment, the numerical model results must be compared with real life data, gathered on site of the pilot area. The variable used for this calibration will be the inside air temperature of each space with measured data. To obtain the values from the TRNSYS simulation, the meteorological data must be organized in a **.txt** file, which will contain in each column the values obtained from the meteorological station on LNEG Campus. New outputs inside of Type 56 will be created to extract the inside air room temperature of each of the ventilated areas, which then will be validated with data gathered from the sensors on-site.

To validate the numerical model, the normalized mean biased error (NMBE) and coefficient of the variation of the root mean square error (cvRMSE) will be used as validation criteria[26].

$$MBE(\%) = \frac{\sum_i^n (S_i - M_i)}{\sum_i^n M_i} \times 100 \tag{4.10}$$

$$RMSE_{period} = \sqrt{\frac{\sum_i^n (S_i - M_i)^2}{m}} \tag{4.11}$$

$$A_{period} = \frac{\sum_i^n M_i}{n} \tag{4.12}$$

$$cvRMSE(\%) = \frac{RMSE_{period}}{A_{period}} \times 100 \tag{4.13}$$

S_i represents the simulated values, M_i the real values, i the time interval and n the number of time intervals for the time period chosen for validation. For a model to be considered validated, NMBE must be in the range of $\pm 5\%$ for monthly calibration and $\pm 10\%$ for hourly calibration, while cvRMSE has to be in the range of $\pm 15\%$ and $\pm 30\%$, respectively.

The validation of the building was done with and without the inclusion of the active systems installed and for the heating and cooling seasons. This implies 4 different validation periods to be analysed:

1. Without active systems, heating season - 22nd of February to 1st of March, 2021.
2. Without active systems, cooling season - 11th to 17th of July, 2021.
3. With active systems, heating season - 16th to 22nd of January, 2023.
4. With active systems, cooling season - 11th to 17th of July, 2022J

For the validation of the pilot area before the renovations took place, the building model described in Section 4.2 had to be adjusted due to some structural changes that happened in the pilot area. These changes influenced the heat loss coefficient of the following surface, which can be seen in Table 4.5

Room	Surface	Change	New U (W/m^2C)	Old U (W/m^2C)
1052/1054	E and W walls	Add another layer of MDF and an airspace of 20cm between the new layer and the old one	0.614	0.407
1052/1054	Ceiling	Replace the ceiling old pasterboard and introduce new boards with an thermal and acoustic insulation	0.882	0.540

Table 4.5: Heat loss coefficient change according to structural renovations in pilot area.

The results of the validation before renovations and without active systems can be seen in Figure 4.5a (for heating period) and Figure 4.5b (for cooling period). The simulation results follow closely the experimental ones, however some discrepancies can be seen - during the heating season, the simulation results are slightly lower than the experimental ones, while during the cooling period the opposite happens. This could be explained by an inaccuracy in the calculation of the infiltration rates or inadequate heat loss coefficients for the wall layers (these values were taken directly from TRNSYS libraries, which do not have the data from manufacturers that originally supplied building materials during construction of Building C).

Nevertheless, the statistical indicators, as seen in Table 4.6 and Table 4.7, fall in the acceptable range and it is possible to assume that the building model properly represents the real building.

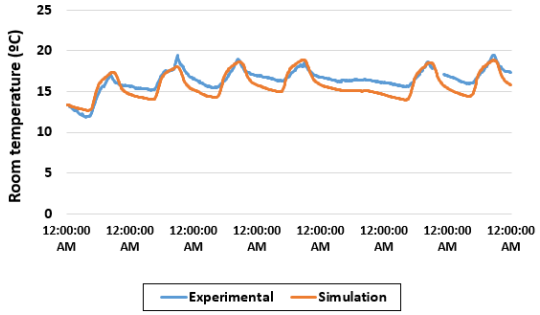

(a) Validation results from heating period with active system for Room 1052.

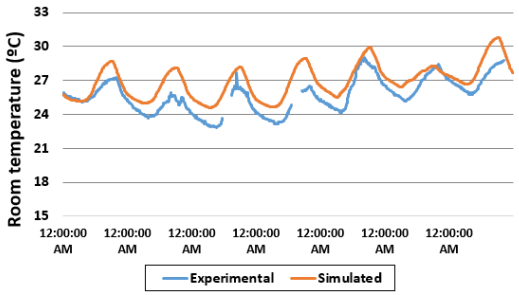

(b) Validation results from cooling period with active system for Room 1054.

Figure 4.5: Validation results of heating and cooling season before renovations.

	22-02	23-02	24-02	25-02	26-02	27-02	28-02
MBE	2.78	-5.42	3.40	-2.77	-7.61	-4.84	-5.31
RMSE	0.67	1.01	0.94	0.98	1.26	1.11	1.22
A	14.33	16.61	16.75	17.07	16.38	16.46	17.24
cvRMSE	4.71	6.10	5.59	5.76	7.68	6.74	7.08

Table 4.6: Statistical indicators for heating period without active systems, room 1052.

	11-07	12-07	13-07	14-07	15-07	16-07	17-07
MBE	2.19	6.59	6.49	6.89	4.08	2.79	4.95
RMSE	0.85	1.76	1.61	1.76	1.14	0.91	1.52
A	25.97	24.63	24.18	24.25	26.40	26.62	26.81
cvRMSE	3.26	7.13	6.64	7.26	4.33	3.43	5.65

Table 4.7: Statistical indicators for cooling period without active systems, room 1052.

Figures 4.6a, 4.6b and 4.6c show the validation results from the cooling season with the active systems turned on. The simulated results follow closely the experimental ones, with small discrepancies due to faulty estimation of the number of occupants and time of occupancy, as well as the setpoint room temperature, which the occupants changed frequently.

The statistical results, summarized in Table 4.8, fall in the acceptable range so the numerical model can be regarded as accurate. The system behaves in a predicted manner, decreasing the temperature during the occupancy schedule to a specified setpoint, and the building thermal behaviour during zero occupancy also has a similar behaviour.

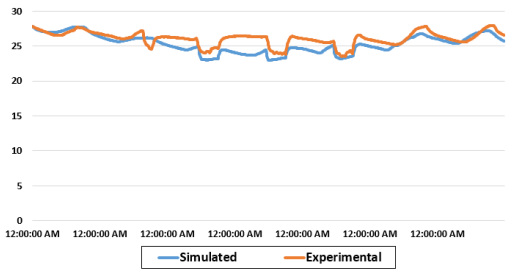

(a) Validation results from cooling period with active system for Room 1052.

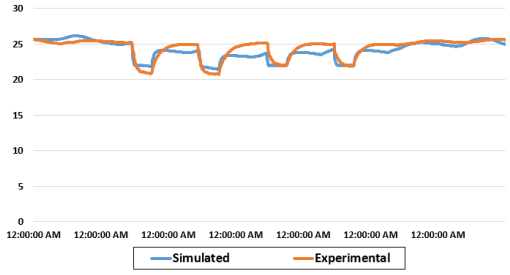

(b) Validation results from cooling period with active system for Room 1054.

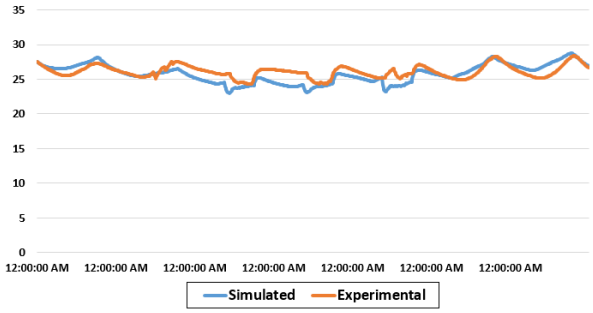

(c) Validation results from cooling period with active system for Rooms 1050.

Figure 4.6: Validation results from cooling season after renovations.

		11-Jul	12-Jul	13-Jul	14-Jul	15-Jul	16-Jul	17-Jul
1052	MBE	0.52%	-1.26%	-5.56%	-7.79%	-4.19%	-2.55%	-1.17%
1054		1.68%	0.68%	-1.20%	-4.08%	-2.87%	-2.05%	-0.77%
1050		2.27%	-1.68%	-5.05%	-5.44%	-3.94%	-5.05%	3.29%
1052	RMSE	0.32	0.72	1.47	1.96	1.14	0.77	0.57
1054		0.51	0.60	0.84	1.24	0.90	0.63	0.39
1050		0.70	0.73	1.41	1.57	1.19	1.597	1.03
1052	A	27.08	26.202	25.586	25.68	25.3415	26.24	26.52
1054		25.35	23.75	23.38	24.00	24.00	25.10	25.42
1050		26.452	26.29	25.67	25.77	25.935	26.23	26.43
1052	cvRMSE	1.18%	2.76%	5.75%	7.63%	4.50%	2.93%	2.16%
1054		2.00%	2.54%	3.60%	5.18%	3.76%	2.50%	1.53%
1050		2.63%	2.79%	5.49%	6.10%	4.58%	6.08%	3.92%

Table 4.8: Statistical indicators of the validation of cooling season with active systems.

Figure 4.7 and 4.8 show the results from the validation during heating season with the active systems on. Unfortunately, there was no occupancy in the room 1050 at the chosen period of time, so the results will only include the rooms which were occupied. Due to a more specific characterization of the occupancy schedules and number of occupants in room 1052 and 1054, the simulation results followed the experimental ones very closely, with the statistical indicators in Table 4.9 showing good accuracy of the numerical model.

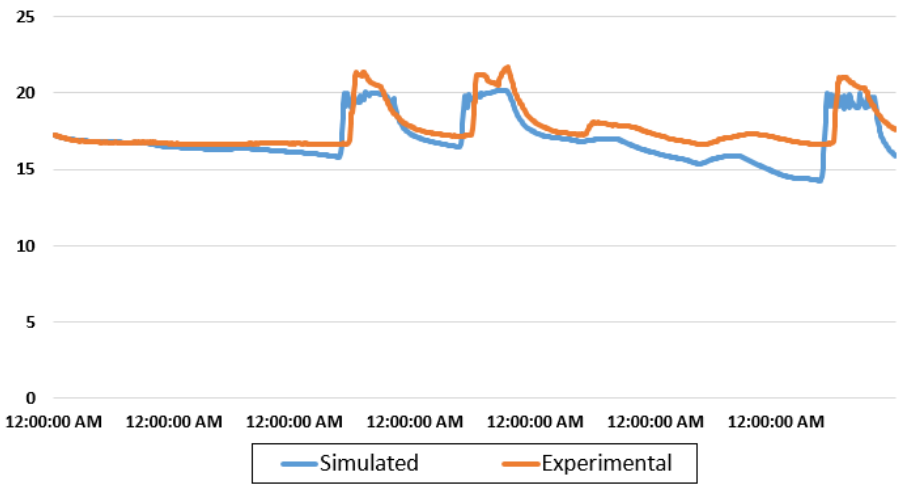

Figure 4.7: Validation results from heating period with active system for Room 1052.

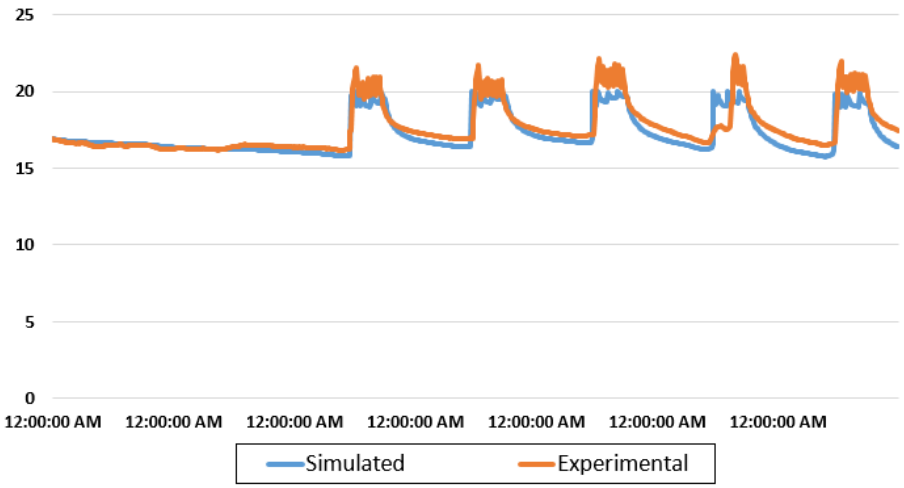

Figure 4.8: Validation results from heating period with active system for Room 1054.

		11-Jul	12-Jul	13-Jul	14-Jul	15-Jul	16-Jul	17-Jul
1052	MBE	-0.11%	-1.37%	-1.33%	-2.25%	-3.22%	-5.40%	-4.63%
1054		0.47%	-0.56%	-1.85%	-1.72%	-2.64%	-1.52%	-3.47%
1052	RMSE	0.096	0.37	1.01	1.07	0.88	1.46	1.88
1054		0.13	0.21	0.68	0.72	0.91	1.082	1.08
1052	A	27.08	26.21	25.58	25.68	25.34	26.25	26.52
1054		25.35	23.75	23.38	24.00	24.00	25.10	25.42
1052	cvRMSE	0.35%	1.41%	3.93%	4.16%	3.47%	5.58%	7.07%
1054		0.53%	0.88%	2.93%	2.98%	3.77%	4.31%	4.26%

Table 4.9: Statistical indicators of the validation of heating season with active systems.

Chapter 5

Experimental results and discussion

The experimental results are relevant to prove the efficacy of the passive and active solutions implemented at the LNEG pilot plant. These can be mainly evaluated by the level of comfort obtained and decrease of energy consumed from the grid.

5.1 Passive solutions

In comparison with the initial construction, the renovations brought several changes, as it can be seen by Table 4.5. To evaluate the efficacy of these implemented solutions, the air temperature of room 1052 will be compared in both configurations.

In order to have a good comparison between two separate periods in time, the meteorological conditions must be similar for both cases. However, it is nearly impossible to find two continuous periods of time, with similar meteorological conditions, from different years. This will introduce some error in the results due to thermal inertial effects of the building, which are difficult to avoid.

5.1.1 Cooling period

2021 - Before renovations		2022 - After renovations		
Day	Mean daily T_{air}	Day	Mean daily T_{air}	Absolute difference
12-07	23.45	20-08	23.49	0.046
13-07	25.44	23-08	25.12	0.318
14-07	25.76	30-08	25.94	0.183
15-07	24.93	16-08	24.98	0.050
16-07	22.70	12-07	22.68	0.022

Table 5.1: Mean outside air temperature.

To compare the effects of passive solutions during the cooling period, two periods of time were chosen, one from the year of 2021 and another from 2022.

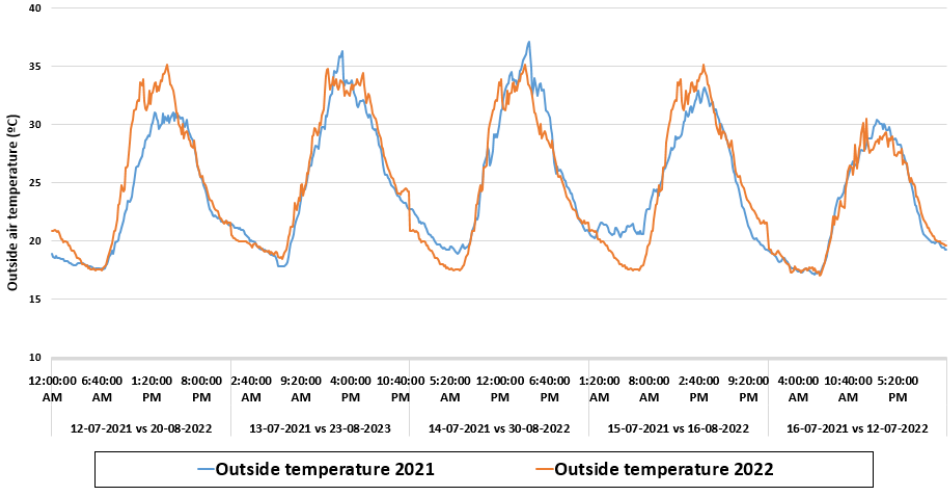

(a) Outside air temperature in 2021 (blue) and in 2022 (orange).

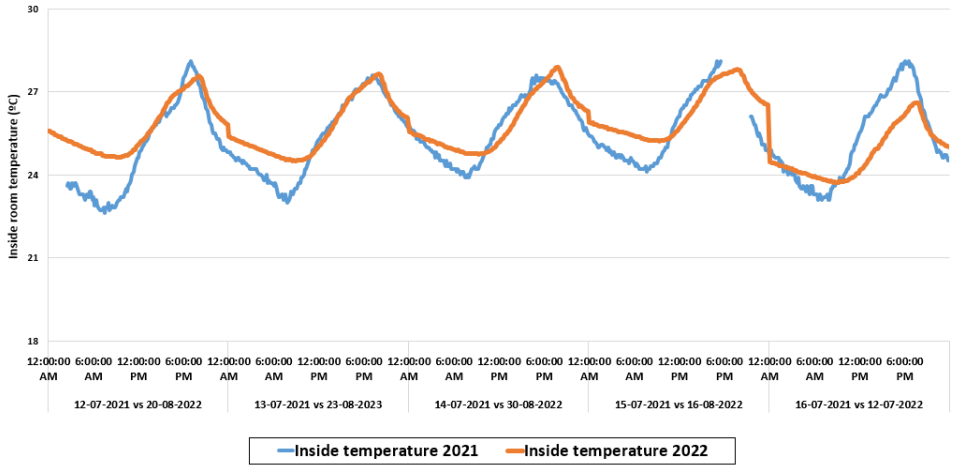

(b) Inside air temperature in 2021 (blue) and in 2022 (orange) of room 1052.

Figure 5.1: Visual representation of passive solutions effect during cooling season in Lisbon at LNEG.

Pre renovation	
Mean	24.45
Standard Deviation	5.17
Sample Variance	26.71

Post renovation	
Mean	24.71
Standard Deviation	5.56
Sample Variance	30.89

Table 5.2: Statistical analysis of outside air temperature in the time periods studied.

Pre renovations	
Mean	25.33
Standard Deviation	1.42
Sample Variance	2.02
Minimum	22.6
Maximum	28.1

Post renovations	
Mean	25.66
Standard Deviation	1.07
Sample Variance	1.14
Minimum	23.73
Maximum	27.88

Table 5.3: Statistical analysis of passive solutions effectiveness according to inside room temperature.

Figure 5.1a shows the proximity of meteorological conditions on both periods of time chosen for the study, while Figure 5.1b shows the experimental data gathered on inside air temperature of room 1052. As seen in Table 5.2, the meteorological conditions are almost identical, with mean air temperature and respective variance very close to each other. As for the passive solutions effectiveness, it can be seen by Table 5.3 that despite the mean values being almost identical, the variance and standard deviations decreased after the implementation of these solutions. As the heat loss of the building envelope decreases in certain areas, it captures more heat during the day, decreasing the maximum temperatures achieved after the peak of solar activity, while at night it releases this heat to the air inside of the room, increasing the minimum temperature during night-time. This lowers the deviation and variance of the air temperature values, leading to more stable temperature levels.

Another measure to evaluate the effectiveness of these passive solutions would be to calculate the thermal energy demand of the space. The equation 5.1 will only take into consideration the thermal demand required to heat the air, without taking into consideration the effects of furniture and walls.

$$Q_{thermal} = m\, C_p\, \Delta T\ = \rho\, V\, C_p\, (T_{setpoint} - T_{air}) \tag{5.1}$$

Using Equation 5.1 and replacing the constant values with the corresponding values for air, the energy demand can be computed for each period. Setting the setpoint temperature of the air, a value of $-291.2\ kWh$ before renovations and $-277.7\ kWh$ after renovations took place, meaning a decrease of approximately 16 % of thermal energy demand.

Since the time period in 2022 chosen for this evaluation is not continuous, the thermal inertial effect can influence the outcome of the results. The dates in 2022 chosen for the comparison are mostly situated in the month of August, one month or more apart from their counterparts. Despite the influence that the thermal inertial effect can have on the building´s thermal behaviour during the first hours of the day, after the peak of radiation at around 12:00PM, this effect can be assumed to follow the meteorological record of the morning hours of those specific days, unaffected by previous days. Thus, the main influence of the passive solutions can be seen with lower temperature decrease during the night.

5.1.2 Heating period

Due to technical issues and timing of the renovation actions undertaken, data is scarce for the heating period when looking for periods of time with equivalent weather conditions. To this effect, only two dates were chosen with similar meteorological conditions to evaluate the effectiveness of the passive solutions during the heating season.

2021 - Before renovations		2022 - After renovations		
Day	Mean daily T_{air} ($^{\circ}C$)	Day	Mean daily T_{air} ($^{\circ}C$)	Absolute difference
6-03	15.40	19-03	15.79	0.389
15-03	15.78	26-03	15.80	0.0259

Table 5.4: Mean outside air temperature.

Before renovations	
Mean	15.79
Standard Deviation	3.996
Sample Variance	15.89

After renovations	
Mean	15.80
Standard Deviation	4.10
Sample Variance	16.78

Table 5.5: Statistical analysis of outside air temperature in the time periods studied.

The meteorological conditions between both periods of time are very similar, as seen by Figure 5.2a as well as Table 5.5. The mean value and variance of outside air temperature is almost identical, but it is important to remember the thermal inertial effect of the building for non-sequential days.

During the heating season, the effect of the passive solutions is much more enhanced, as the deviation and variances - seen in Table 5.6 - greatly decrease after the renovations were finished. This implies a great deal of thermal stability to the pilot area, maintaining a steady temperature as seen in Figure 5.2b.

As for the energy demand, using Equation 5.1 the decrease in energy demand is around 23 %, proving again the efficacy of these solutions.

Before renovations	
Mean	17.20
Standard Deviation	1.394
Sample Variance	1.95
Minimum	14.7
Maximum	20.4

After renovations	
Mean	17.97
Standard Deviation	0.63
Sample Variance	0.40
Minimum	16.82
Maximum	19.30

Table 5.6: Statistical analysis of passive solutions effectiveness according to inside room temperature.

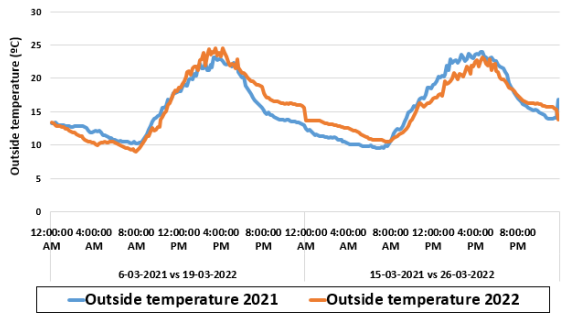

(a) Outside air temperature in 2021 (blue) and in 2022 (orange).

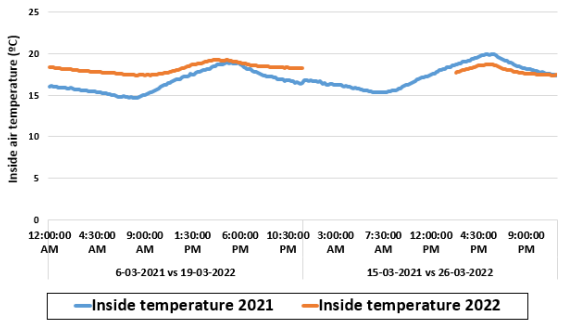

(b) Inside air temperature in 2021 (blue) and in 2022 (orange) of room 1052.

Figure 5.2: Visual representation of passive solutions effect during the heating season.

It is important to notice that in both Figure 5.1 and Figure 5.2 exist discontinuities in data when it comes to the measures inside air temperature. This can be explained by some technical constraints posed by the instrumentation. These constraints, such as lack of sensors charge and the data back-up from the data logger, would coincide esporadically with times where it would be impossible to implement these manual procedures. This would lead to some gaps in the collected data from the order of minutes to a couple of hours.

5.2 Electric consumption

The main definition of an nZEB building is to consume as much energy as it is produced. To evaluate whether this goal was met with the LNEG pilot plant, the data from the electric components were analysed for the period from 9^{th} of March of 2022 up until the 6^{th} of February of 2023.

The consumption can be organised into several categories:

1. Fan coil - E_{FC}.
2. Heat pump - E_{HP}.
3. Lights of rooms 1050 and 1052 - E_{lights}.
4. Always on equipment - controllers of heat pump and fan coils - E_{ON}.
5. Others + power socket of room 1050 - E_{other}.

To compute the value of total consumption of the pilot area, it is necessary to add the electric consumption of the heat pump to the energy supplied to the microgrid - E_{supply}. This has to be done due to the fact that the heat pump is a three-phase equipment and there was no possibility to connect it to the pilot area grid due to time constraints.

To compute the value of E_{other}, the following equation must be put to use:

$$E_{other} = E_{supply} - E_{FC} - E_{lights} \tag{5.2}$$

To find the value of the consumption of the controller for the fan coils and heat pump, the data for power consumption was filtered to only include values below a very low value, when compared with the nominal power of these machines. These values - $E_{FC}^{control}$ and $E_{HP}^{control}$ - will be subtracted to E_{FC} and E_{HP}, respectively, in order to compute the exact value of energy consumption of the equipments without the controllers.

In the end,the amount of energy left aside is the consumption of other equipments. The process will also filter the data into the working and the non working period consumption - working period includes the time period from 8:00 AM to 8:00 PM during workdays.

Looking at Fig.5.3, the main consumer of energy in the pilot area is the heat pump, representing almost 50% of total consumption. Interestingly, the ”Always-on” and ”Other” energy represent a large share of the consumption, with a total of 40% for both categories. This illustrates that there is a lot of idle equipments constantly turned on to the power source, as well a very low occupancy throughout the year of the analysed rooms. Despite the fact that controllers and other equipment have a very low power consumption in comparison to the heat pump and fan coils, as they are turned on 100% of the time, the cumulative energy of these small contributions surpasses the contribution of the higher rated equipments.

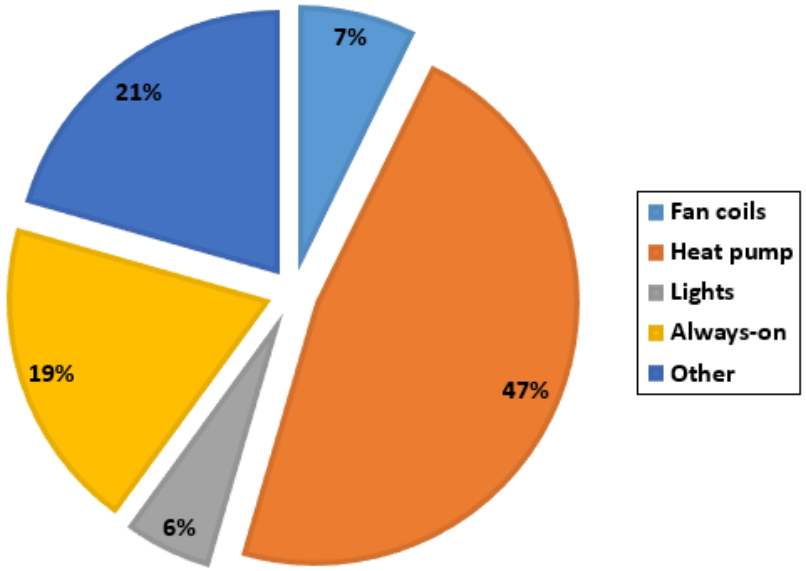

Figure 5.3: Consumption percentage of the different sub-systems in LNEG pilot area.

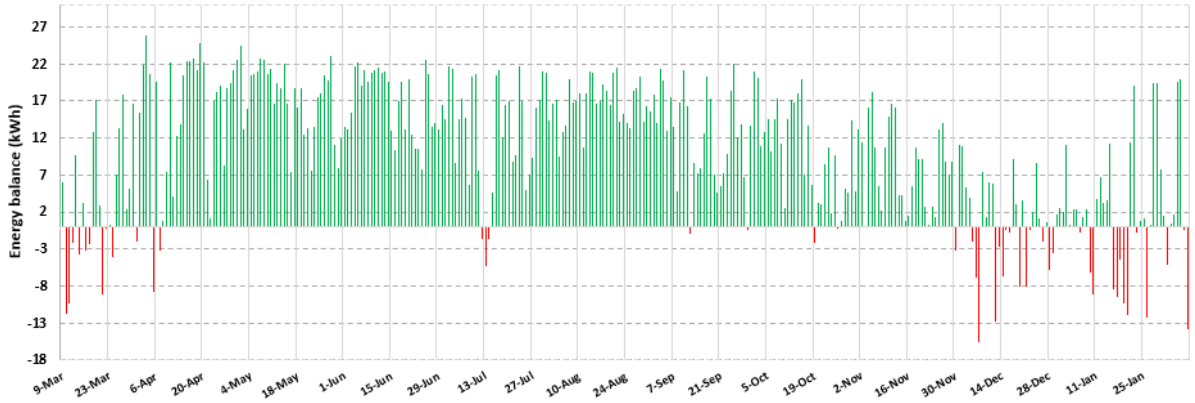

Figure 5.4: Surplus and shortage graph from March 2022 up to February 2023.

As such, there will be many days during the year with a surplus of energy. By doing a daily analysis, as it can be seen in Figure 5.4, production exceeds consumption 86% of the time.

Looking at Fig. 5.5, the assumption made earlier about the low occupancy rates can be justified as well. It is important to notice that in the beginning a small mistake was made in the programming of the heat pump which greatly raised the consumption levels - the heat pump was turned on during the night, which prompted this equipment to work extra hours with no purpose.

Throughout the year, there is a constant consumption cycle, which represents a normal week cycle for an office. This can be explained by the consumption in the room 1050, which had a very regular occupancy schedule. In some specific parts of the year, which were coincidental with project meeting and big conferences that took place in rooms 1052 and 1054, the consumption almost quadrupled, thus decreasing the surplus of energy. Special attention must be put in the last weeks of 2022 and first weeks

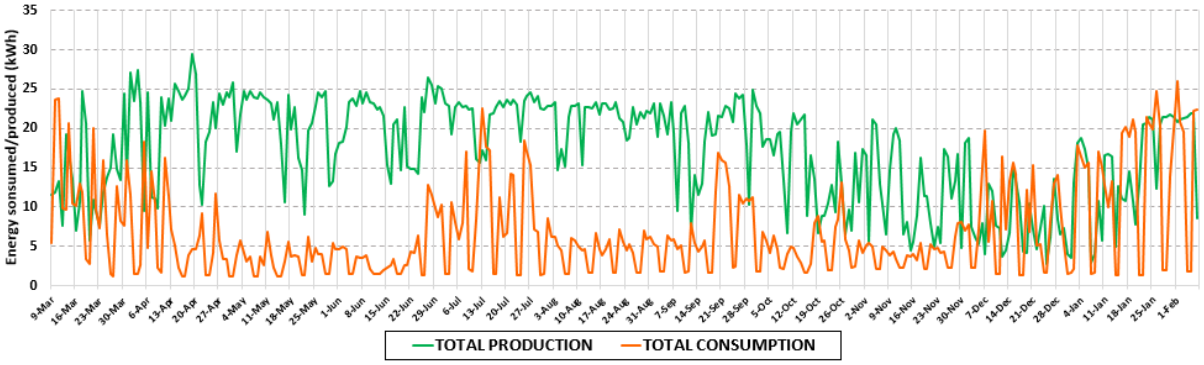

Figure 5.5: Daily production vs consumption graph.

of 2023 - due to regular testing of the pilot area, with or without occupation (meaning that the ventilation system would be turned on every day), the amount of days with surplus energy decreased drastically, leading to a large portion of days with a shortage of energy.

5.3 Economic and Direct Mode

As mentioned previously, the system of the LNEG pilot area can run in economic or direct model. To prove any advantages that the direct mode can have over the economic, it is important to compare the consumption of the heat pump and fan coils in two similar meteorological periods, for each of the configurations.

Due to the inability to find similar meteorological periods of time for the heating season, only the results from the cooling season will be shown.

To validate whether the meteorological periods are identical a *t-Test: Paired Two Samples for Means* tool of Excel was used. According to this test, both these time periods are well adjusted are similar to each other.

	Variable 1	Variable 2
Mean	25.38	24.85
Variance	21.23	15.97
P(T<=t) one-tail	4.11E-07	
P(T<=t) two-tail	8.22E-07	

Table 5.7: Statistical comparison between study periods.

As the one-tail and two-tail p-tests are lower than than 0.05, it can be concluded that these time periods are statistically comparable. The heat pump and fan coil consumption were plotted and compared one to another.

Both the economic and direct configurations have a peak of consumption in the beginning of the day in order to pre-cool the water in the mixture tanks - although the direct mode does not specify a setpoint temperature for the water, the fan coils require the temperature to reach a certain level in order to operate efficiently. As such, since the inertial tank has a larger volume than the smaller mixture tank, the initial

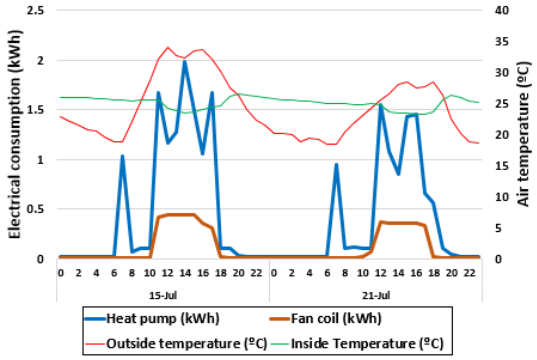

(a) Economic mode electric consumption consumption, outside and inside air temperature.

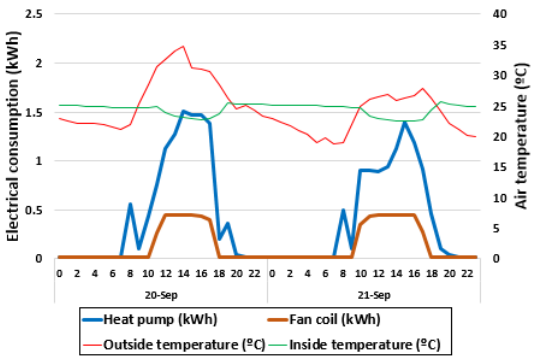

(b) Direct mode electric consumption consumption, outside and inside air temperature.

Figure 5.6: Economic vs direct mode comparison.

peak of consumption is lower for the direct mode than for economic one. The profile of consumption is also evidently much different: the direct mode has a steady consumption of energy, that rises with the demand for cooling as the exterior temperatures rise, while the economic mode has several peaks of consumption throughout the day in order to meet the required setpoint temperature in the tank.

Although the profile heat pump has several differences, the fan coil consumption profile is very similar.

	Summer	
	Direct (kWh)	Eco (kWh)
HP total	20.51	21.31
FC total	6.73	5.32
TOTAL	27.25	26.63
Improve	0	-2.3 %

Table 5.8: Electric consumption comparison between economic and direct modes.

The difference between both configurations is minimal, with a 2.3 % advantage for the economic mode. It is also important to notice that the cooling period matches the period with the highest monthly irradiation, which could mean that entire energy demand, electrical and thermal, could be met with RES.

5.4 Solar fraction in economic mode

One of the measure to evaluate the effectiveness of the solar sub-system integrated into the climatization system is the solar fraction, which represents the percentage of heat that is delivered to the inertial tank by the heat exchanger, Q_{HX}, divided by the total heat delivered, which is the sum of Q_{HX} with Q_{HP}, corresponding to the heat delivered by the heat pump.

$$f_{solar} = \frac{Q_{HX}}{Q_{HX} + Q_{HP}} \tag{5.3}$$

In the month of January, regular testing was performed with the system in economic mode with as-

sistance of the solar system. As this is one the coldest periods during the year, it was a good opportunity to prove the performance of the system during extreme temperatures.

Using Equation 5.3, the values of Q_{HX} and Q_{HP} were taken from the enthalpy meters readings, E3 and E2 respectively. The results show that the heat pump contributed with $0.837\ MWh$ of thermal energy, while the solar system only contributed with around $0.107\ MWh$. This bring the solar fraction to around $11.33\ \%$, which could be perceived as very low levels of solar fraction.

Chapter 6

Numerical Model Results

Key Performance Indicators, or KPI´s, are quantities largely used in many areas, such as business, engineering and others, to analyse the performance of several factors. In the case of the LNEG pilot area, it is of interest to analyse the system when it comes to the comfort levels inside [27], but also in regards to the technical performance of the equipments [28].

For the purpose of this work, a list of variables was chosen to perform a parametric study and to analyse the evolution of the KPI´s according to them.

1. Volume of inertial tank - 600, 1000 and 1500 L were the volumes chosen, all related to tanks from the same series as for the installed model. To better adjust the simulation results, the height of the tanks was introduced as an auxiliary variable, $H_{inertia}$ (accordingly, $H_{inertia}$ = [1.73 ; 2.25 ; 2.32])

2. Setpoint temperature of inertial tank - Depending on the season, different setpoint temperatures for the inertial tank had to be chosen. For winter, the range was [40; 43; 45; 47; 50] and for summer [8; 10; 12; 14; 16]

3. Room setpoint temperature - The setpoint temperature also changed according to the season - for winter the range was [18; 19; 20; 21; 22] and for summer [21; 22; 23; 24; 25]

6.1 Technical KPI´s

6.1.1 Thermal energy savings

For passive solutions in the pilot area, a KPI called Thermal Energy Savings was used. This shows the variation in thermal energy required to heat/cool the pilot area - in the respective seasons - compared to a reference case, which was chosen to be the pilot area before the renovations took place.

$$TES(\%) = \left(1 - \frac{E_i}{E_{ref}}\right) \times 100 \tag{6.1}$$

E_{ref} represents the energy required to heat/cool the space for the reference case, while E_i represents all the case studies presented in the following list:

1. Reference case (meaning that TES = 0)
2. Renovated pilot area
3. Renovated pilot area with triple glass and argon filled windows
4. Renovated pilot area, with better windows and 10cm woolrock insulation on E and W walls
5. Renovated area, with better windows, 10cm woolrock insulation on E and W walls and very low infiltration rate (0.1 ARH)

All these reference cases will be calculated separately for the heating and cooling season, in order to access the magnitude of implementation of certain passive solutions in the heating and cooling seasons. In the TRNBUILD environment, it is possible to define a ”Heating” and ”Cooling” type. For each time interval, depending on the difference between the room temperature and a pre-defined set-point temperature, the software calculates and ideal heating/cooling energy that needs to be supplied so that air inside keeps at a pre-defined level [29].

In Table 6.1 the total thermal energy demand from all the rooms in the pilot area are presented, excluding the hallway which has no need to have temperature control. The reference setpoint temperature used as input to the TRNSYS simulation was $20°C$ for heating season and $24°C$ for the cooling period. In this simulation, only the

	Cooling (kWh/m^2year)	TES	Heating (kWh/m^2year)	TES
Case 1	40.86		104.02	
Case 2	41.20	1%	67.95	-35%
Case 3	26.98	-34%	75.42	-27%
Case 4	28.91	-29%	66.73	-36%
Case 5	41.09	1%	28.76	-72%

Table 6.1: Total heating and cooling energy demand for a whole year, with corresponding energy savings compared to Case 1.

Figure 6.1 illustrates how the passive measures can influence the energy demand in the LNEG pilot area. For the heating season, by implementing additional measures, the energy demand decreases substantially, reaching a value of 72% of less energy demand. However, for the cooling season, the trend is completely different - as the passive solutions are improved, the demand for cooling does not change much, reaching a maximum saving of around 34% for Case 3.

During the heating season, it is necessary to retain the heat inside of the building to avoid heat losses to the exterior. As the passive solutions improve, the losses decrease and with the additional thermal gains from the people inside and all the equipments, the heating demand decreases.

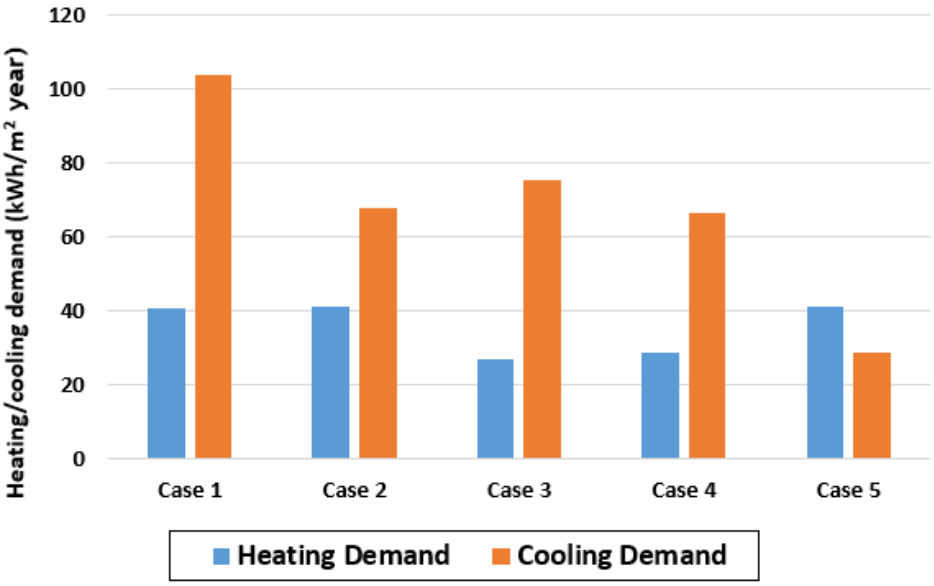

Figure 6.1: Total thermal energy demand for a yearly period

During the cooling season, the gains inside of the building have a contrary effect on the air temperature and conditions inside. As the losses decrease, there is less transfer of energy between the exterior and interior, but despite the changes the building will eventually heat itself due to exterior and also interior gains. This combination of gains increases substantially the cooling demand - the values presented in Table 6.1 show a lower total for cooling rather than for heating, but this is due to the short amount of time that the building actually requires cooling due to atmospheric conditions, which happens usually from June up until September.

If the building design is made for colder climates, it makes sense to have thick insulation, extremely low air leakage and the best windows on the market. However, for hotter climates, it becomes an issue during summer, as it will drive the investment cost for a remodelled building very high - more passive solutions means more cooling demand, which leads to more capacity of cooling needed.

6.1.2 Solar fraction

This KPI focuses on calculating the percentage of thermal energy that is supplied by RES sources. Despite having several different definitions, the expression for the computation of this quantity is the following:

$$f_{solar} = \frac{Q_{HX}}{Q_{HX} + Q_{HP}} \tag{6.2}$$

Q_{HP} represents the energy supplied by the heat pump to maintain the setpoint temperature of the inertial tank at the setpoint, while Q_{HX} relates to the energy transferred from the solar tank to the inertial tank through the heat exchanger. It is important to notice that this KPI can only be evaluated for the heating period, as in the cooling season the solar sub-system is shut-off from the inertial tank.

The goal of using the solar fraction is to evaluate its variation depending on the room setpoint temperature, the inertial tank setpoint temperature and volume. The first variable relates to the demand of

energy from the inertial tank, while the next ones relate to the maximum amount of thermal energy that can be stored.

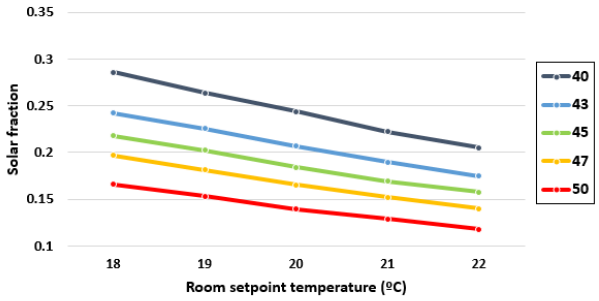

Figure 6.2: Solar fraction evolution for $V_{inertia} = 1000L$.

	18	19	20	21	22
40	0.286	0.264	0.244	0.222	0.205
43	0.242	0.226	0.207	0.190	0.175
45	0.218	0.202	0.184	0.169	0.157
47	0.197	0.181	0.165	0.152	0.140
50	0.166	0.153	0.139	0.129	0.118

Table 6.2: Solar fraction values for $V = 1000L$ (left-side column refers to room setpoint temperature in $^{\circ}C$ and top-row refers to inertial tank setpoint temperature in $^{\circ}C$).

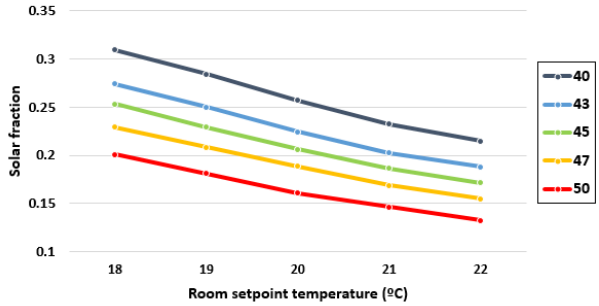

Figure 6.3: Solar fraction evolution for $V_{inertia} = 600L$.

	18	19	20	21	22
40	0.310	0.284	0.257	0.233	0.215
43	0.274	0.250	0.224	0.202	0.188
45	0.253	0.229	0.206	0.186	0.171
47	0.229	0.208	0.188	0.169	0.155
50	0.201	0.181	0.161	0.146	0.132

Table 6.3: Solar fraction values for $V = 600L$ (left-side column refers to room setpoint temperature in $^{\circ}C$ and top-row refers to inertial tank setpoint temperature in $^{\circ}C$).

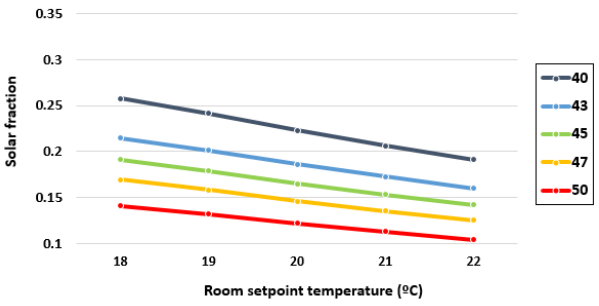

Figure 6.4: Solar fraction evolution for $V_{inertia} = 1500L$.

	18	19	20	21	22
40	0.258	0.241	0.223	0.206	0.191
43	0.214	0.201	0.186	0.173	0.160
45	0.191	0.179	0.165	0.153	0.142
47	0.169	0.158	0.146	0.135	0.125
50	0.141	0.132	0.122	0.113	0.104

Table 6.4: Solar fraction values for $V = 1500L$ (left-side column refers to room setpoint temperature in $^{\circ}C$ and top-row refers to inertial tank setpoint temperature in $^{\circ}C$).

According to the previous graphs and tables, the optimal volume of the inertial tank is $600\ L$. As the solar tank volume remains the same, the heat it can exchange with the inertial tank remains the same,

however the increase in mean temperature will decrease as the volume of the inertial tank goes up. If the conditions for the activation of the solar circuit are met (Equation 4.2), to raise $T_{inertia}$ one degree, the solar tank will lose $2°C$ for $V_{inertia} = 600L$, while for $V_{inertia} = 1500L$ the solar tank will lose $5°C$ (this assuming that the solar tank is not receiving energy from the sun).

With the increase of volume the solar tank alone will take more time to heat up the tank, as the heat transfer rate is fixed by the constant speed of the pump connecting the solar system to the inertial tank. However, the heat pump also activates with the same condition as the solar system (Equation 4.3), with the only difference being the second condition for the solar system, which states that the temperature in the solar tank must be superior than that of the inertial one. With both these systems working together, as volume of the inertial tank increases, it becomes increasingly difficult to heat the tank only with solar energy and the heat pump starts to have a bigger impact on the temperature increase.

It is noticeable a decrease of the solar fraction with the increase of the setpoint temperature. Due to the meteorological conditions, the solar system can have more or less production of energy according to the time of the year and the heating season is the period where it produces less energy than the rest of the year. During the night, the tank also loses a lot of energy, which can be recovered - or not - to the tank, so the probability that the temperatures will surpass higher setpoint temperatures decreases. As the condition for the activation of the solar system is met less times, the heat pump has a bigger impact on maintaining the setpoint temperature of the tank, which decreases the solar fraction substantially.

The variation according to the room setpoint temperature also follows the same behaviour. As the heating demand increases (defined by the setpoint temperature), the inertial tank loses more energy each time the fan-coils are triggered to activate. This increase also implies that the energy collected from the solar system will soon be depleted and the heat pump will have a higher energy consumption due to this.

6.1.3 Seasonal Coefficient of Performance

The definition of SCOP is defined by the International Energy Agency (IEA), but depending on the configuration and the purpose of the study its computation will vary according to the system´s boundaries defined.

In order to study the efficiency of the cooling and heating systems, the chosen boundary was SHP_{bSt}, which corresponds to the solar heat pump system without storage, meaning that it only quantifies the performance up until the storage tank, excluding the climatization system.

$$SCOP = \frac{Q_{SH}}{E_{SH}} = \frac{Q_{HP} + Q_{HX}}{E_{pump}^{solar} + E_{HP}} \tag{6.3}$$

According to Equation 6.3, the heat supplied is a sum of the solar contribution, Q_{HX} with the heat pump delivered energy, Q_{HP}. As for the electrical energy supplied to operate this subsystem, the solar pumps (primary and secondary), E_{pump}^{solar} and the heat pump E_{HP} electric consumption is included.

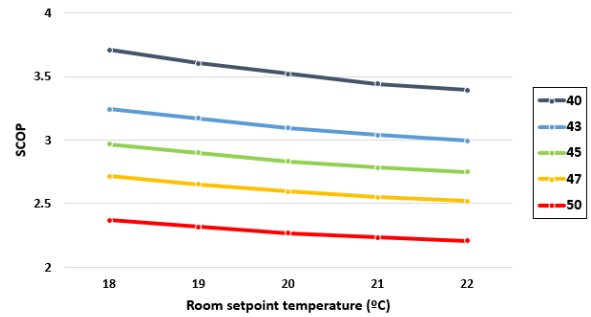

Figure 6.5: SCOP evolution for $V_{inertia} = 1000L$.

	18	19	20	21	22
40	3.710	3.605	3.522	3.442	3.392
43	3.243	3.171	3.097	3.040	3.000
45	2.969	2.900	2.832	2.785	2.751
47	2.716	2.653	2.594	2.552	2.519
50	2.370	2.318	2.269	2.236	2.207

Table 6.5: Values of SCOP for $V_{inertia} = 1000L$ (left-side column refers to room setpoint temperature in $^{\circ}C$ and top-row refers to inertial tank setpoint temperature in $^{\circ}C$).

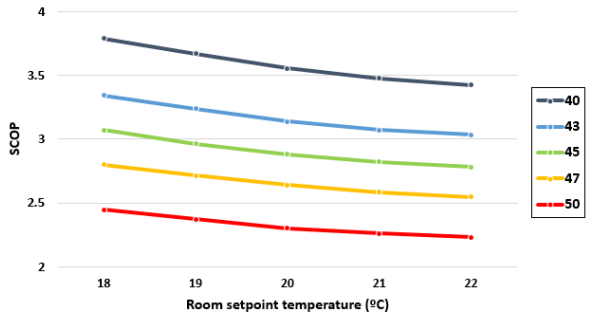

Figure 6.6: SCOP evolution for $V_{inertia} = 600L$.

	18	19	20	21	22
40	3.790	3.670	3.556	3.475	3.424
43	3.343	3.238	3.138	3.070	3.032
45	3.071	3.138	2.883	2.822	2.783
47	2.800	3.070	2.640	2.585	2.549
50	2.448	3.032	2.304	2.262	2.230

Table 6.6: Values of SCOP for $V_{inertia} = 600L$ (left-side column refers to room setpoint temperature in $^{\circ}C$ and top-row refers to inertial tank setpoint temperature in $^{\circ}C$).

Figure 6.7: SCOP evolution for $V_{inertia} = 1500L$.

	18	19	20	21	22
40	3.593	3.519	3.442	3.384	3.338
43	3.146	3.089	3.031	2.985	2.948
45	2.880	2.827	2.776	2.739	2.707
47	2.633	2.588	2.543	2.509	2.481
50	2.303	2.266	2.229	2.200	2.176

Table 6.7: Values of SCOP for $V_{inertia} = 1500L$ (left-side column refers to room setpoint temperature in $^{\circ}C$ and top-row refers to inertial tank setpoint temperature in $^{\circ}C$).

The performance of the system has a similar behaviour for the solar fraction, as the maximum SCOP also occurs at the lowest inertial tank and room temperature setpoints. This can be explained by the power ratings of the heat pump and of the solar pump. More solar fraction means that the heat pump is activated less time - as it has a considerable difference of power consumption from the solar pump, a decrease of ”on” time for the heat pump has a bigger effect on the summatory with the consumption of

the solar pump, whose power rating is approximately 100 times lower.

6.1.4 Seasonal Energy Efficiency Ratio

The definition of SEER will follow the same system boundary as in the previous. The cooling energy will only be supplied by the heat pump, Q_{HP}, while the energy input will include the electrical consumption of the heat pump, E_{HP}, as well as of the renovation system, E_{renov}.

$$SEER = \frac{Q_{SC}}{E_{SC}} = \frac{Q_{HP}}{E_{HP}} \tag{6.4}$$

The computation of the SEER will follow the same logic as for SCOP, but in this case there is no "free-cooling" available to the system, so only the heat pump consumption will be evaluated.

The variation of this KPI is not significant when it comes to volume nor room setpoint temperature. However, when changing the setpoint temperature of the inertial tank, the efficiency of the system in cooling mode increases. As the heat pump operates with inlet water coming from the inertial tank, the lower the difference in water coming into the heat pump and out of it, the more efficiently it operates. By changing the setpoint temperature, there is less difference between the temperature of the water and the room temperature, so the water increases the temperature more slowly. This can be explained by the decrease in Carnot efficiency of the cycle. It is also important to notice that in Figures 6.8, 6.9 and 6.10 the curves for inertial tank setpoint temperature of 8 and 10$°C$ are almost coincidental and thus creates some interference between both curves - this suggest some saturation of results for very low values of inertial tank setpoint temperatures.

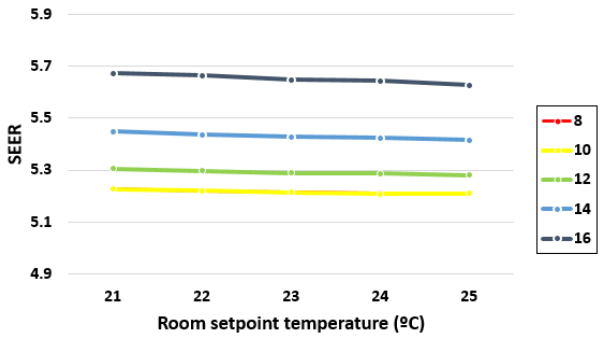

Figure 6.8: SEER evolution for $V_{inertia} = 1000L$.

	8	10	12	14	16
21	5.23	5.23	5.31	5.45	5.67
22	5.22	5.22	5.30	5.44	5.66
23	5.21	5.21	5.29	5.43	5.65
24	5.21	5.21	5.29	5.42	5.64
25	5.21	5.21	5.28	5.41	5.63

Table 6.8: Values of SEER for $V_{inertia} = 1000L$ (left-side column refers to room setpoint temperature in $°C$ and top-row refers to inertial tank setpoint temperature in $°C$).

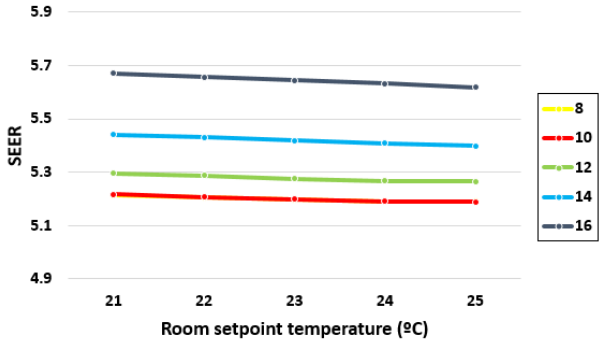

Figure 6.9: SEER evolution for $V_{inertia} = 600L$.

	8	10	12	14	16
21	5.21	5.22	5.30	5.44	5.67
22	5.21	5.21	5.29	5.43	5.66
23	5.20	5.20	5.28	5.42	5.64
24	5.19	5.19	5.27	5.41	5.63
25	5.19	5.19	5.26	5.40	5.62

Table 6.9: Values of SEER for $V_{inertia} = 600L$ (left-side column refers to room setpoint temperature in $^{\circ}C$ and top-row refers to inertial tank setpoint temperature in $^{\circ}C$).

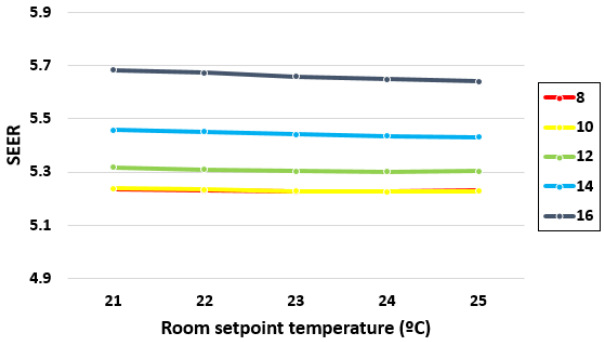

Figure 6.10: SEER evolution for $V_{inertia} = 1500L$.

	8	10	12	14	16
21	5.24	5.24	5.32	5.46	5.68
22	5.23	5.23	5.31	5.45	5.67
23	5.23	5.23	5.30	5.44	5.66
24	5.23	5.23	5.30	5.44	5.65
25	5.23	5.23	5.30	5.43	5.64

Table 6.10: Values of SEER for $V_{inertia} = 1500L$ (left-side column refers to room setpoint temperature in $^{\circ}C$ and top-row refers to inertial tank setpoint temperature in $^{\circ}C$).

6.1.5 Seasonal Performance Factor

The seasonal performance factor is a metric that defines the performance of the whole system for a period of a year. To compute this quantity, the following equation must be used:

$$SPF = \frac{Q_{SC} + Q_{SH}}{E_{SC} + E_{SH}} \tag{6.5}$$

Q_{SC} refers to the thermal energy used for space cooling, while Q_{SH} refers to the heating and the indexes E_{SC} and E_{SH} refer to the energy supplied, accordingly. In order to simplify the analysis due to the large number of variable combinations that could be made, only the inertial tank setpoint temperature in the reference case were used ($T^{winter}_{setpoint} = 45$ and $T^{summer}_{setpoint} = 14$). The value for the room setpoint temperature were chosen according to its difference to the mean ambient temperature of the season, in descending order:

1. Winter - as temperatures are colder, the first value for room setpoint is 22, decreasing to 18.
2. Summer - as temperatures are hotter, the first value for room setpoint is 21, increasing up until 25.

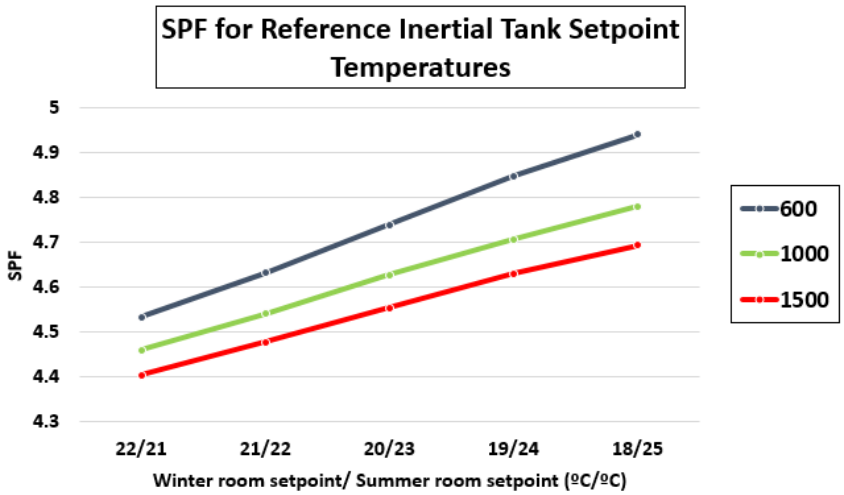

Figure 6.11: SPF of the LNEG pilot area system for $V = 600L, 1000L$ and $1500L$.

As the difference to the mean ambient temperature decreases, either in summer or winter, the system operates under more optimal conditions, as seen by Figure 6.11. This means that during winter is more optimal to decrease the setpoint temperature and in summer is better to increase it, which results in lower heating/cooling demands, respectively.

6.2 Comfort

One of the main goals of the SUDOE IMPROVEMENT project was to also guarantee comfort conditions. To measure how well the project achieved these objectives, two variables were chosen - *PMV* (Predicted Mean Vote) and *PPD* (Percent People Dissatisfied) - which are widely used to evaluate the levels of thermal comfort in various spaces [30].

The *PMV* is used to predict a mean value of votes for a specific occupancy, which is organized on a 7 point thermal sensation scale. The equation that computes this variable is a function of two personal parameters - clothing insulation (I_o in clo) and metabolic rate (M) - as well as four environmental ones - air temperature (T_{air} in $^\circ C$), radiant temperature (T_{rad} in $^\circ C$), air velocity (V_{air} in m/s) and relative humidity (R_h in %).

$$PMV = f(I_o, M, T_{air}, T_{rad}, V_{air}, R_h) \tag{6.6}$$

The thermal sensation scale has 7 levels: -3 (very cold), -2 (cool), -1 (slightly cool), 0 (neutral), +1 (slightly warm), +2 (warm), +3 (hot). ISO 7730 puts the hard limit on this parameter between -2 and +2, but for more precise definition it must be at least between -1 and +1. As for the personal parameters of the Equation 6.6, I_o was fixed at 1 clo, which is a representative value for full formal attire (socks, formal suit, shirt, shoes) and M was fixed at around 125W per person, which according to EN 13779 represents stationary activity in an office. Fortunately, TRNSYS has an option to compute these coefficients as outputs of the simulation, however, only the midpoint in each room was analysed for these parameters, which will only prove thermal comfort in one area of the room, instead of the whole space.

For simplification, only room 1052 was analysed for thermal comfort, as it is the biggest room and also because it has the largest amount of people inside when occupied.

The PPD is a function of PMV, which shows shows the level of satisfaction of the occupants according to the personal and environmental parameters.

$$PPD = 95\ \exp\left(-0.003353\ PMV^4 - 0.2179\ PMV^2\right) \tag{6.7}$$

By computing these comfort KPI´s for the previous parametric study, the variation of these variables according to the inertial tank setpoint temperature was insignificant, as well as for the variation in volume. Due to this, only one configuration for each season will be shown.

1. Winter - $V_{inertia} = 1000L$, $T_{inertia}^{setpoint} = 45$.
2. Summer - $V_{inertia} = 1000L$, $T_{inertia}^{setpoint} = 12$.

For the cooling season, the thermal comfort is achieved almost all the time. Most PMV values lie in the zone between neutral and slightly warm sensation, while PPD is mostly below 20%. With the increase in temperature, the PMV and PPD show more thermal discomfort for same clothing and metabolic rate. It is interesting to notice some occurrences between slightly cold and neutral sensation, which could be associated with the thermal shock when the ventilation system is activated in a hot room.

As for the heating season, thermal discomfort is felt all throughout the season, as most values for PMV lie between cold and slightly cold sensation, while PPD shows high levels of dissatisfaction for all room setpoint temperatures. However, with the increase of room setpoint temperature, a higher thermal comfort can be achieved according to Figure 6.14b, but the changes are almost minimal.

The results for comfort are calculated every 15 seconds, which is the step of the simulation. However, it is not important to evaluate comfort levels during the night-time, as well as during the weekend, so these values were filtered out and not taken into consideration. The values on the vertical axis represent the number of occurrences for each range of PPD and PMV values.

In order to evaluate the effect of different clothing for the heating and cooling periods, two new simulations were made with I_o better adjusted for each of the seasons. For summer, a value of 0.7 clo was chosen, which corresponds to a combination of trousers, short-sleeved shirt, short socks and shoes. For winter, a value of 1.2 clo was chosen, corresponding to a combination of T-shirt, knee socks, trousers, sweatshirt and jacket, all made specifically for winter weather.

The change of the clothing insulation factor I_o, has made considerable changes for summer time comfort values as seen in Figures 6.13. First, the percentage of PMV values inside of the comfort zone (between ”neutral and slightly warm”) has remained almost unchanged, but the percentage of PMV values in the zone of ”slightly cold to neutral” has increased substantially. This change was possible due to a decrease in values located in the ”slightly warm to warm” region, which means that the occupants will feel a ”chilly” sensation more often than with the previous clothing ensemble.

Nevertheless, the PPD values have improved greatly and most of the measurements lie on the range of [0, 20], which means a low level of dissatisfaction through most of the cooling season.Moreover, there

is a higher level of stability when changing from one room setpoint temperature to another, which means high levels of comfort for any room conditions that the occupants choose to be in.

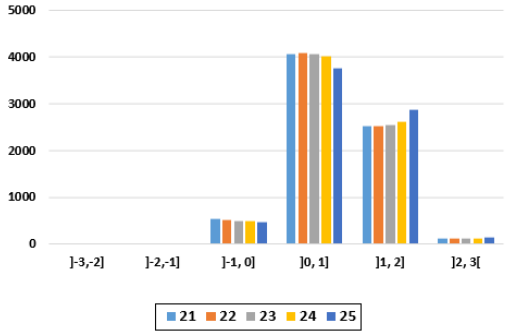

(a) PMV results from cooling season room 1052.

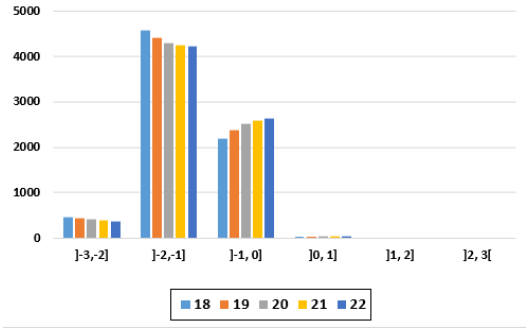

(b) PMV results from heating season room 1052.

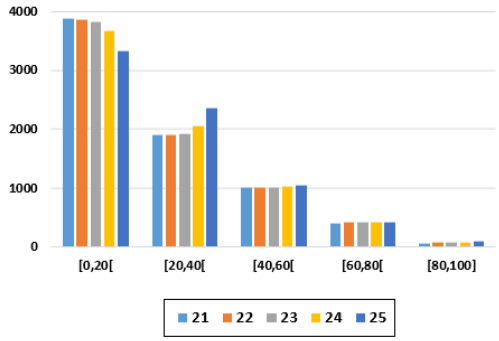

(c) PPD results from cooling season room 1052.

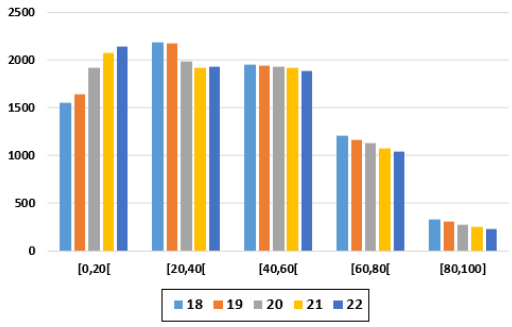

(d) PPD results from heating season room 1052.

Figure 6.12: Comfort KPI results for $V_{inertia} = 1000L$, $T_{inertia}^{setpoint} = 45$ (winter) and $T_{inertia}^{setpoint} = 12$ (summer).

When using the same analysis for the heating season, with the new $I_o = 1.2$, the changes are even more pronounced, as can be seen by Figure 6.14. By looking at the PMV, there is a major improvement of thermal comfort, as most of the values lie in the ”slightly cold to neutral” zone, which can be identified as comfortable. But the confirmation of better comfort conditions can be identified by the PPD graph, which shows a much lower percentage of dissatisfied people compared to the previous clothing ensemble. With the increase of room setpoint temperature, a slight improvement of comfort conditions can be identified.

However, this analysis takes into consideration stationary metabolic rates, which can be slightly inaccurate when one looks at the transitory changes on skin temperature, that occur when working for long periods of time [31]. Furthermore, one could argue that due to different clothing insulation of the various parts of the body (for example, the difference between the feet and torso), the thermal sensation on the different parts could be different. And that might be true, either because of different clothing insulation, or by any thermal effects of the ventilation or the building itself.

Nevertheless, this analysis was based on a very stationary mode of work, in which the metabolic rate will not change greatly in relation to time. To reduce the uncertainty due to different clothing insulation factors in separate parts of the body, special care was taken to adjust the clothing ensemble in each of the season to have an approximately equal insulation factor all throughout the body.

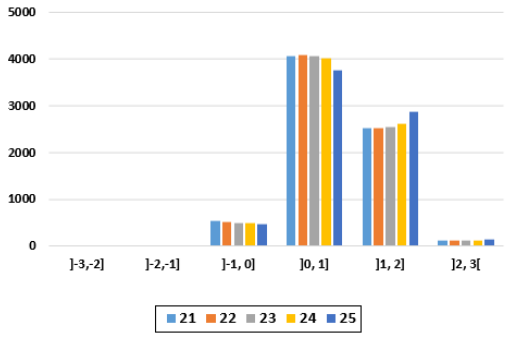

(a) PMV results from cooling season with $I_o = 1$.

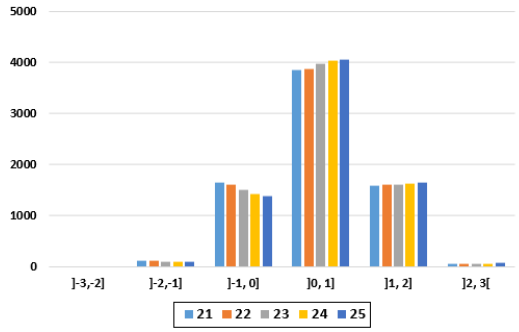

(b) PMV results from cooling season with $I_o = 0.7$.

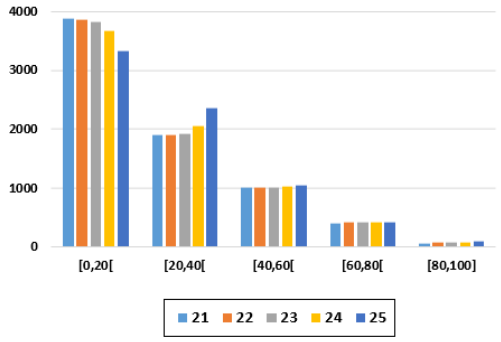

(c) PPD results from cooling season with $I_o = 1$.

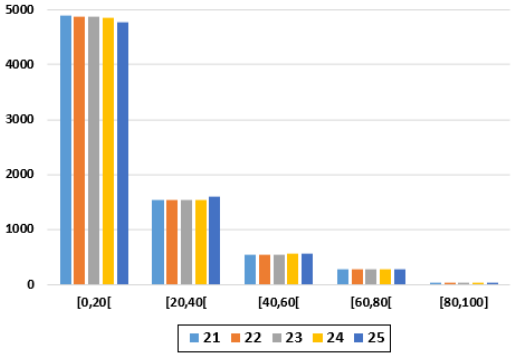

(d) PPD results from cooling season with $I_o = 0.7$.

Figure 6.13: Comfort KPI results for $V_{inertia} = 1000L$, $T^{setpoint}_{inertia} = 45$ (winter) and $T^{setpoint}_{inertia} = 12$ (summer).

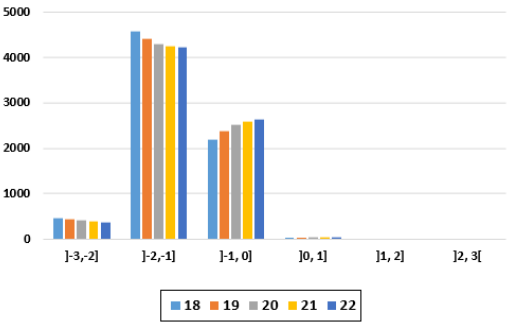

(a) PMV results from heating season with $I_o = 1$.

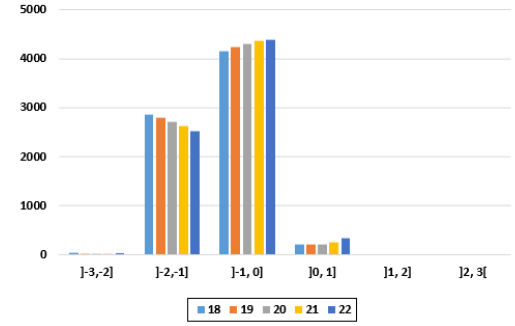

(b) PMV results from heating season with $I_o = 1.2$.

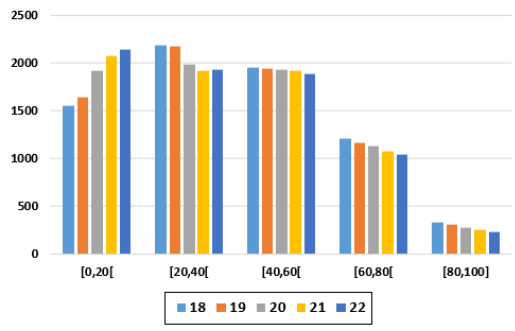

(c) PPD results from heating season with $I_o = 1$.

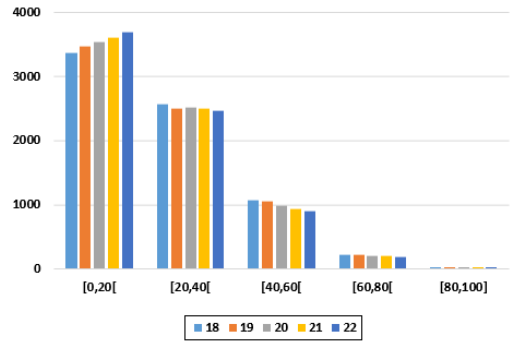

(d) PPD results from heating season with $I_o = 1.2$.

Figure 6.14: Comfort KPI results for $V_{inertia} = 1000L$, $T^{setpoint}_{inertia} = 45$ (winter) and $T^{setpoint}_{inertia} = 12$ (summer).

Chapter 7

Conclusions

7.1 Achievements

The goal of this work was to analyse the performance of the installation on the pilot area of the Building C of the Lumiar LNEG Campus, either by looking into experimental data gathered on site or simulation results, which were the product of numerical model in TRNSYS software. A number of objectives were achieved, such as:

1. Detailed characterization of the LNEG pilot area and the renovations that took place.
2. Description of the climatization system installed, with all the sub-systems.
3. Description of the monitoring system.
4. Analysis of the passive and active solutions installed on the pilot area with resource to experimental data.
5. Creation of numerical model in TRNSYS, subsequent validation with experimental data and analysis of performance according to specified KPI´s.

Due to technical issues, there was a significant difficulty in gathering enough experimental data from the pilot area in order to evaluate the improvements in all the seasons. Nevertheless, with the values that were gathered, some conclusions were taken, such as:

1. The passive solution improved thermal behaviour of the inside air temperature, either in heating or cooling season, reducing thermal demand in 23% and 16% respectively. Despite these improvements, other solutions could have been implemented, such as installation of new windows and the construction of double brick walls on the East and West side, which could not have been realised due to legal reasons.
2. If the climatization system is not being actively used, a lot of energy is lost in ”idle” operation, such as controllers and ”always-on” equipment. This means that a tighter management of energy should be put in place, with a system that could turn on and off entire sub-systems with regards

to a pre-defined occupancy schedule or momentary demand. However, this would require the purchase of more electronic parts to the heat pump and fan-coils, which due to financial reasons were not possible to include in the project.

3. In similar meteorological conditions during the cooling season, the economic mode has little difference between the direct one in cooling mode, which counts as a disadvantage of the RES integration. The insignificant energy demand decreases and significantly more costly and complex system makes the economic configuration a less desirable option.

4. The contribution of the solar system during heating season is very low, at around 11 % of total thermal energy needs. This could be explained by either two factors: there is not enough solar collectors, or the control strategy is not tuned for optimal operation of the solar sub-system. The control for the heat pump and the solar sub-system activates both when $T_{inertia}$ is 1 degree lower than the setpoint temperature - as both systems activate at the same time, the heat pump has a more instantaneous contribution to increase the temperature in the inertial tank, which leaves lees time for the operation of the solar sub-system.

When it comes to results from the numerical model, some major conclusions can be taken:

1. Passive solutions are highly effective during the heating period, but during the cooling season they might not have the desired effect. The increase of quality of passive solutions has a positive effect during the heating season, however it can have a negative effect during cooling season, as it can create a sort of ”greenhouse” effect inside of the room, which can increase cooling demand from one case to the other. Nevertheless, all these improvements have a positive effect compared to the reference case, which proves the low thermal performance of the building envelope before renovations.

2. Solar fraction and SCOP improve with the decrease of inertial tank volume and setpoint temperature, as well as with room setpoint temperature. Optimal tank sizing could be approximately equal to the solar tank or even lower, which would improve heat exchange between these systems. The tank setpoint temperature must be maintained at a specific temperature level, which is around 40$^{\circ}C$, required by the manufacturers of fan-coils, which puts a hard-limit on how much the setpoint temperature can be decreased to improve performance. As for room temperature, lower temperatures would only mean more uncomfortable conditions, which could be only improved by an increased amount of clothing insulation.

3. During cooling season, the performance only increases with the increase of the inertial tank setpoint, while being practically unchanged regarding the other two variables. Despite this behaviour, this temperature is also limited by the fan-coil manufacturers due to performance issues.

4. The yearly performance of the system can be improved with the decrease of the differential between the room setpoint temperature and the mean ambient temperature, as well as of the inertial tank volume. This would mean a lower setpoint in winter and higher setpoint in summer, which

would require an adaptation of clothing insulation of the occupants to achieve better thermal comfort.

7.2 Future Work

This study had some limitations, which blocked the possibility to better study the performance of the installed systems, such as:

1. Late completion of the entire installation, which left a very short amount of time for uninterrupted testing and data collection.
2. Disconnected battery storage system, which does not provide information about self-consumption and self-sufficiency of the installation, both important metrics to evaluate off-grid systems.

Despite these set-backs, the installation has been completed by the end of March, in the year of 2023, which can lead to some future work such as:

1. Analysis of system´s performance with the connected battery system, with a clear definition and scheduling of tests throughout the year for different configurations.
2. Improvement of the EMS to avoid losses of energy due to idle equipment.
3. Load management of non-prioritary loads.
4. Creation of a software tool for scheduling of occupancy in order to estimate the daily heating and cooling needs.

Bibliography

[1] I.E.A., "World energy outlook 2022, IEA, Paris https://www.iea.org/reports/world-energy-outlook-2022, License: CC by 4.0 (report)," *CC BY NC SA*, vol. 4.0. Annex A.

[2] T. Wilberforce, A. Olabi, E. T. Sayed, K. Elsaid, H. M. Maghrabie, and M. A. Abdelkareem, "A review on zero energy buildings–Pros and Cons," *Energy and Built Environment*, vol. 4, no. 1, pp. 25–38, 2023.

[3] E. E. Commission), "Energy, transport and environment statistics," 2020.

[4] F. Martins, P. Moura, and A. T. de Almeida, "The role of electrification in the decarbonization of the energy sector in portugal," *Energies*, vol. 15, no. 5, 2022.

[5] "Net zero energy buildings: A consistent definition framework," *Energy and Buildings*, vol. 48, pp. 220–232, 2012.

[6] "Law decree, n. 98/2019." Building Energy Certification System.

[7] "Energy, economic and environmental benefits of integrating passive design strategies into buildings: a review," *Renewable and Sustainable Energy Reviews*, vol. 167, 2022.

[8] "Hybrid renewable energy system for sustainable residential buildings based on solar dish stirling and wind turbine with hydrogen production," *Energy Conversion and Management*, vol. 270, 2022.

[9] L. E. Aelenei, H. Gonçalves, and C. Rodrigues, "The road towards "zero energy" in buildings: lessons learned from SOLARXXI building in portugal," in *EUROSUN 2010 International Conference on Solar Heating, Cooling and Buildings*, 2010.

[10] S. A. Kalogirou, "Building integration of solar renewable energy systems towards zero or nearly zero energy buildings," *International Journal of Low-Carbon Technologies*, vol. 10, no. 4, pp. 379–385, 2013.

[11] "Advancements of wind energy conversion systems for low-wind urban environments: A review," *Energy Reports*, vol. 8, pp. 3406–3414, 2022.

[12] R. Liu, M. Salem, J. Rungamornrat, and M. Al-Bahrani, "A comprehensive and updated review on the exergy analysis of ground source heat pumps," *Sustainable Energy Technologies and Assessments*, vol. 55, p. 102906, 2023.

[13] M. D. Hossen, M. F. Islam, M. F. Ishraque, S. A. Shezan, and S. Arifuzzaman, “Design and implementation of a hybrid solar-wind-biomass renewable energy system considering meteorological conditions with the power system performances,” *International journal of photoenergy*, vol. 2022, 2022.

[14] “A review on anaerobic digestion with focus on the role of biomass co-digestion, modelling and optimisation on biogas production and enhancement,” *Bioresource Technology*, vol. 344, p. 126311, 2022.

[15] A. Estanqueiro, A. Joyce, L. E. Aelenei, J. Facão, C. Rodrigues, D. Loureiro, J. Teixeira, J. B. Correia, Á. Ramalho, S. Camelo, *et al.*, “Conversão de edifícios existentes em nZeb através da integração de energias renováveis, de micro-redes e de soluções de eficiência energética,” in *CIES2020-XVII Congresso Ibérico e XIII Congresso Ibero-americano de Energia Solar*, pp. 987–995, LNEG-Laboratório Nacional de Energia e Geologia, 2020.

[16] A. Cavaco, H. Silva, P. Canhoto, S. Neves, J. Neto, and M. Collares Pereira, “Annual average value of solar radiation and its variability in portugal,” 2016.

[17] “Instituto Mortuguês do Mar e Mtmosfera.” Acessed on 21/03/2023.

[18] “BAXI.” Acessed on 15/03/2023.

[19] “BAXI.” Acessed on 15/03/2023.

[20] “DAITSU.” Acessed on 15/03/2023.

[21] “LAPESA.” Acessed on 15/03/2023.

[22] G. Pagliarini, C. Corradi, and S. Rainieri, “Hospital CHCP system optimization assisted by TRNSYS building energy simulation tool,” *Applied Thermal Engineering*, vol. 44, pp. 150–158, 2012.

[23] M. Wetter and C. Haugstetter, “Modelica versus TRNSYS - a comparison between an equation-based and a procedural modeling language for building energy simulation,” *Proceedings of SimBuild*, vol. 2, no. 1, 2006.

[24] M. Rashad, A. Żabnieńska-Góra, L. Norman, and H. Jouhara, “Analysis of energy demand in a residential building using TRNSYS,” *Energy*, vol. 254, p. 124357, 2022.

[25] A. Athienitis, M. Stylianou, and J. Shou, “A methodology for building thermal dynamics studies and control applications,” *ASHRAE Transactions (American Society of Heating, Refrigerating and Air-Conditioning Engineers);(United States)*, vol. 96, no. CONF-9006117-, 1990.

[26] E. Fabrizio and V. Monetti, “Methodologies and advancements in the calibration ofbuilding energy models.”

[27] A. Fratean and P. Dobra, “Key performance indicators for the evaluation of building indoor air temperature control in a context of demand side management: An extensive analysis for romania,” *Sustainable Cities and Society*, vol. 68, p. 102805, 2021.

[28] S. Díaz de Garayo, A. Martínez, and D. Astrain, “Annual energy performance of a thermoelectric heat pump combined with a heat recovery unit to HVAC one passive house dwelling,” *Applied Thermal Engineering*, vol. 204, p. 117832, 2022.

[29] M. Rashad, A. Żabnieńska Góra, L. Norman, and H. Jouhara, “Analysis of energy demand in a residential building using TRNSYS,” *Energy*, vol. 254, p. 124357, 2022.

[30] S. Zhang, W. He, D. Chen, J. Chu, H. Fan, and X. Duan, “Thermal comfort analysis based on PMV/PPD in cabins of manned submersibles,” *Building and Environment*, vol. 148, pp. 668–676, 2019.

[31] H. Wang, Z. Xu, B. Ge, and J. Li, “Experimental study on a phase change cooling garment to improve thermal comfort of factory workers,” *Building and Environment*, vol. 227, 2023.